Execution and reliability of slip resistant connections for steel structures using CS and SS (SIROCO)

Report To: RFCS
Document: Literature Study on Creep and Stress Relaxation of Stainless Steel at Room Temperature
Version: 01
Date: December 2016

Version	Date of Issue	Purpose	Author	Technical Reviewer	Approved
01	31.12.2016	Issue to RFCS and TGS8	TPM	LEA	MYl

The testing, assessment, findings and conclusions outlined in this report have been made with the intent of due diligence, care and best effort. Neither Outokumpu nor the authors of this report may be held liable for any direct, compensatory or consequential loss or damage suffered as a result of recommendations, forecasts, judgments, conclusions or any course of action determined based on this report.

EUROPEAN COMMISSION

Research Programme of
The Research Fund for Coal and Steel - Steel RTD

Title of Research Project:	**Execution and reliability of slip resistant connections for steel structures using CS and SS (SIROCO)**
Executive Committee:	**TGS8**
Contract:	**RFSR-CT-2014-00024**
Commencement Date:	**July 01, 2014**
Completion Date:	**June 30, 2017**
Work Package No and Title:	**WP5, Preloading of SS bolts**
Deliverable No and Title:	**5.1, Report on available material data**
Report title:	**Literature Study on Creep and Stress Relaxation of Stainless Steel at Room Temperature**
Beneficiaries:	**Outokumpu Stainless Oy** **FI-95490 Tornio, Finland** **Outokumpu Stainless AB** **SE-77422 Avesta, Sweden**
Research Locations:	**Outokumpu Stainless Oy** **Tornio R&D Center** **FI-95490 Tornio, Finland** **Outokumpu Stainless AB** **Avesta R&D Center** **SE-77422 Avesta, Sweden**
Contact person:	**Dr. Leeni Aula,** **Outokumpu Stainless Oy** **FI-95490 Tornio, Finland**
Report authors:	**Timo Manninen,** **Emma Jakobsen,** **Johan Pilhagen**

2016_0051
2016-12-29
Technical report
Published

Literature Study on Creep and Stress Relaxation of Stainless Steel at Room Temperature

Timo Manninen, Emma Jacobsen, Johan Pilhagen

Abstract

A literature study was conducted to review and collect the published information on creep and stress relaxation behavior of stainless steel at room temperature. The characteristics of creep and stress relaxation behavior of different types of stainless steels is discussed. Also mathematical models with potential for describing the creep deformation in preloaded slip-resistant bolted connections made of stainless steel are reviewed.

Key words: Literature study, room temperature, creep, stress relaxation, austenitic stainless steel, ferritic stainless steel, duplex stainless steel, SIROCO -project

Approved by: Leeni Aula

Contents

1. Introduction

Creep deformation is defined as the time-dependent inelastic strain that occurs when material is subjected to sustained loading [1]. In contrast to plastic flow, creep can occur also when stresses are below the yield strength of the material. Although creep deformation can occur at any temperature, creep deformations of crystalline solids such as metals and ceramics are typically very small if the service temperature is below $0.5\ T_m$, where T_m is the melting temperature in Kelvin scale. Therefore creep is typically considered to be a high temperature phenomenon. [1–3]

The temperature ranges for creep of metals and engineering alloys are conventionally divided into three categories:

High temperature creep ($T/T_m > 0.6$).
Intermediate temperature creep ($0.3 < T/T_m < 0.6$).
Low temperature creep ($T/T_m < 0.3$).

Most creep studies have been concentrated in high temperature deformation. The creep at low temperatures has received less attention since structures "generally neither fail nor experience large creep deformations at low temperatures". [4]

Creep characteristics of materials are normally studied by creep testing. Creep testing involves subjecting a tensile specimen to constant stress at constant temperature and measuring the elongation with time. A schematic illustration of a creep curve measured at high homologous temperature ($T/T_m > 0.6$) is shown in Figure 1. Based on the shape of the curve, the material behaviour is conventionally divided in three stages termed primary or transient creep, secondary or steady state creep and tertiary or accelerating creep.

The primary creep follows after the application of the load. In this stage the creep rate gradually decreases. After certain period of time, the rate eventually reaches a constant steady state value. The stage in which rate of creep deformation is nearly constant is known as secondary creep. Finally microstructural damage, e.g. in the form of voids and microcracks, begins to accumulate and the rate of creep deformation again continues to increase. The third state known as tertiary creep usually precedes the failure of the specimen. [3,5,6]

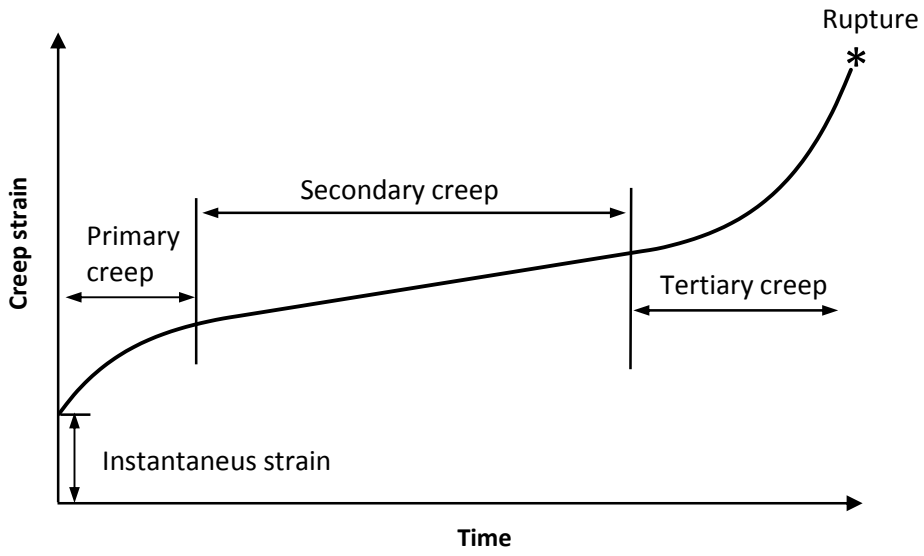

Figure 1. Schematic illustration of creep curve measured at high temperature.

At low temperature and low stress the creep curve exhibits only the transient stage characterized by a creep rate that decreases with time, Figure 2. The observed creep strain often obeys an empirical equation of the form

$$\varepsilon = \alpha \ln t \quad \Leftrightarrow \quad \dot{\varepsilon} = \frac{\alpha}{t} \qquad (1)$$

This kind of creep behaviour is called α-creep or logarithmic creep. Already in 1951 Wyatt has shown that the low temperature transient creep of annealed pure metals is of logarithmic type [7].

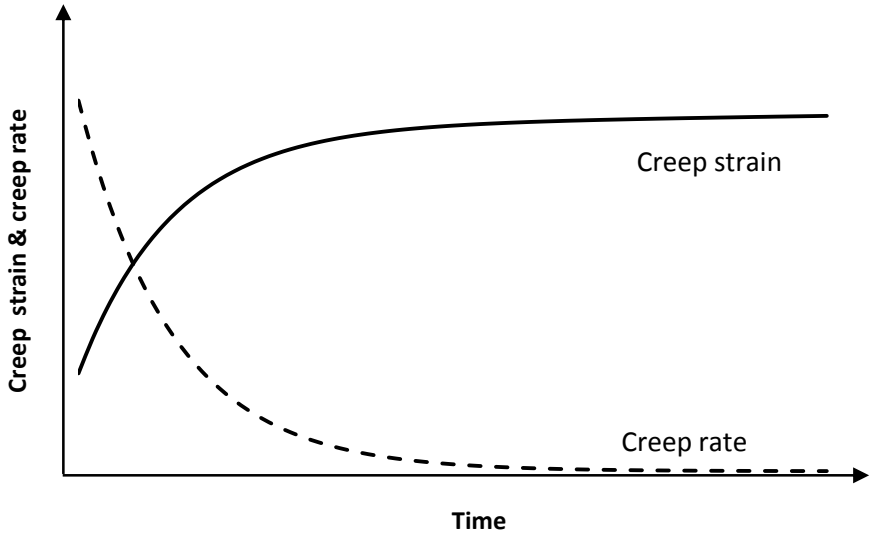

Figure 2. Schematic illustration of a low temperature creep curve.

2. Deformation mechanisms for low temperature transient creep

According to Frost and Ashby [8], five different deformation mechanisms may cause permanent (inelastic) deformations in metals.

1. Collapse by separation of crystal planes when the theoretical shear strength of crystal lattice is exceeded.
2. Low-temperature plasticity by dislocation glide. The stress required to cause slip by dislocation motion depends on the strength by which different obstacles such as precipitates and solute atoms resist the movement of dislocations.
3. Low temperature plasticity by twinning
4. Power-law creep by dislocation glide or by glide and climb.
5. Diffusional creep by lattice diffusion or by diffusion of atoms along grain boundaries. These two creep processes are also known as Nabarro-Herring creep and Coble creep, respectively.

Different deformation mechanisms dominate at different ranges of temperature and stress. The region of dominance of each mechanism can be presented in the form of deformation mechanism map [8] . Figure 3 shows the deformation mechanism map for type AISI 316 austenitic stainless steel. Figure 4 shows the deformation mechanism map for Fe-9Cr ferritic-martensitic steel. The region relevant for creep and stress relaxation of stainless steel in preloaded slip resistant connections is indicated by a small rectangle in both figures. Based on the Ashby deformation maps, it can be concluded that low- temperature plasticity by dislocation glide is the physical mechanism responsible for the creep and stress relaxation of stainless steel at room temperature. It follows that the rate at which the creep process advances depends on the strength and spacing of different barriers dislocation motion existing in the material, and on the rate by which dislocations are able to surmount the obstacles assisted by thermal activation.

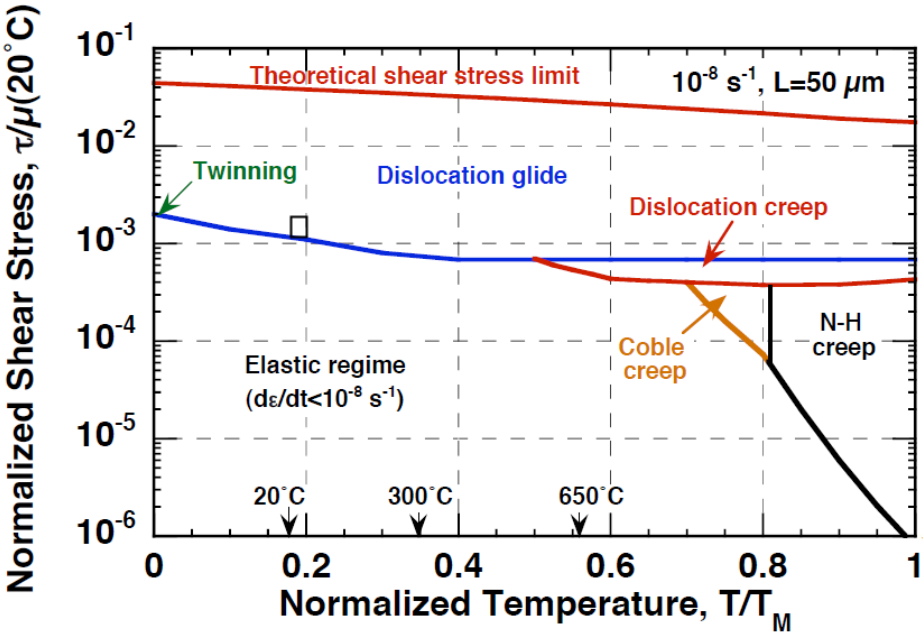

Figure 3. Deformation mechanism map for AISI type 316 austenitic stainless steel, adapted from [9] . The region for room temperature creep in slip resistant connections is indicated by small rectangle.

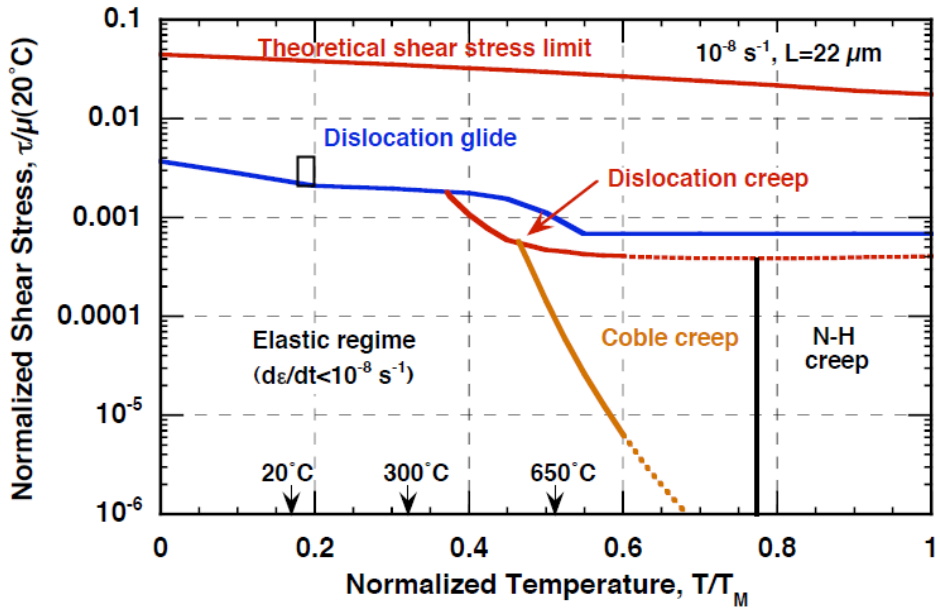

Figure 4. Deformation mechanism map for type Fe-9Cr ferritic-martensitic steel, adapted from [9]. The region relevant for room temperature creep in slip resistant connections is indicated by small rectangle.

In metal physics the logarithmic creep law described by equation (1) has been explained by two competing theories: the strain hardening theory [10] and the exhaustion theory [11]. Short summaries of both theories are given by Nabarro [12,13]. Both theories explain the decreasing creep rate by thermally activated movement of dislocations over different types of barriers.

The strain hardening theory [10] studies the influence of thermal fluctuations on the dislocation motion in a strain hardening material. The stress-strain behaviour of a strain hardening material during a creep test is illustrated in Figure 5. In the beginning of the test, the application of the load OA produces an instantaneous strain AP. The applied stress is enough to produce only the strain AP; any increase beyond this value would require an increase of stress. The dislocations are trapped at energy barriers, for example at the sites of impurity atoms or precipitates. However, as soon as the instantaneous extension has ceased at point P, thermal fluctuations begin surmounting the dislocations over the barriers. As a result of this process creep begins, and the strain increases beyond AP. During the creep deformation the external load remains constant whereas the activation stress increases continuously due to strain hardening. It follows that when the creep strain has increased to PQ, the barrier that needs to be surmounted by thermal activation equals to QR.

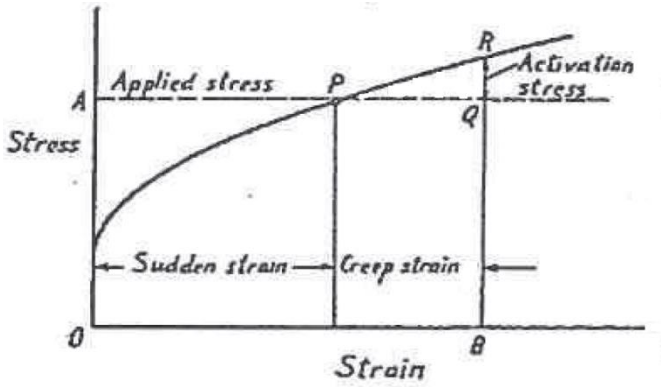

Figure 5. Schematic illustration of strain hardening material in creep test. Adapted from [11].

Under the small strains involved, the activation energy *U* can be expressed as a linear function of height of the barrier

$$U = U_0 - V(\sigma - h\varepsilon_c) \tag{2}$$

where *h* is the work hardening rate and ε_c is the creep strain. The parameters U_0 and V describe the activation energy and the derivative of the activation energy with respect to the activation stress evaluated at point P.

Since the movement of dislocations occurs through thermal activation, rate of creep deformation is given by

$$\dot{\varepsilon}_c = \dot{\varepsilon}_0 \exp\left(-\frac{U}{kT}\right) \tag{3}$$

where k is the Boltzmann coefficient. Substituting (2) in (3) gives

$$\frac{d\varepsilon_c}{dt} = \dot{\varepsilon}_0 \exp\left(-\frac{U_0 - V(\sigma - h\varepsilon_c)}{kT}\right) \tag{4}$$

Integrating (4) and taking into account the boundary conditions finally yields

$$\varepsilon_c = \frac{kT}{Vh} ln\left(1 + \frac{t}{t_0}\right) \tag{5}$$

where

$$t_0 = \frac{kT}{Vh\dot{\varepsilon}_0} \exp\left(\frac{U_0 - V\sigma}{kT}\right) \tag{6}$$

The resulting creep deformation is therefore of logarithmic type.

In the competing exhaustion theory it is assumed that the activation energies of barriers are continuously distributed over a range from zero upwards. The dislocation segments attack each barrier with a frequency which equals to the vibration frequency of a dislocation segment of about 100 atoms long. The frequency of these lattice vibrations is extremely high, of order 10^{10} Hz. It follows that the weaker obstacles are quickly surmounted. This produces the rapid creep in the beginning of the test. However, as the process continues, further creep deformation can only occur by surpassing the stronger barriers. Thermal fluctuations capable of doing this are rare, and consequently, the creep rate falls. Several analyses have shown that this process also leads to logarithmic creep [11,12,14].

The significance of these early theories is that they correctly identify mechanisms which are controlling the rate of creep deformation at room temperature.

3. Creep deformation

Mechanics is the part of physics that studies the movement and deformation of matter. In the field of mechanics, the deformations are conventionally classified in different categories according to Figure 6. In this classification system room temperature creep is termed viscoplastic deformation or viscoplasticity.

The term viscoelasticity has been occasionally used to describe creep and the resulting stress relaxation in rebar and pre-stressing tendons. This is misuse of the term since the deformation in question will hardly vanish upon unloading. Genuine viscoelastic behaviour is observed in polymers, rubbers, concrete, wood and other biomaterials. In structural metals deformed at room temperature, however, the time-dependent elastic deformation is negligible compared to the other components [15].

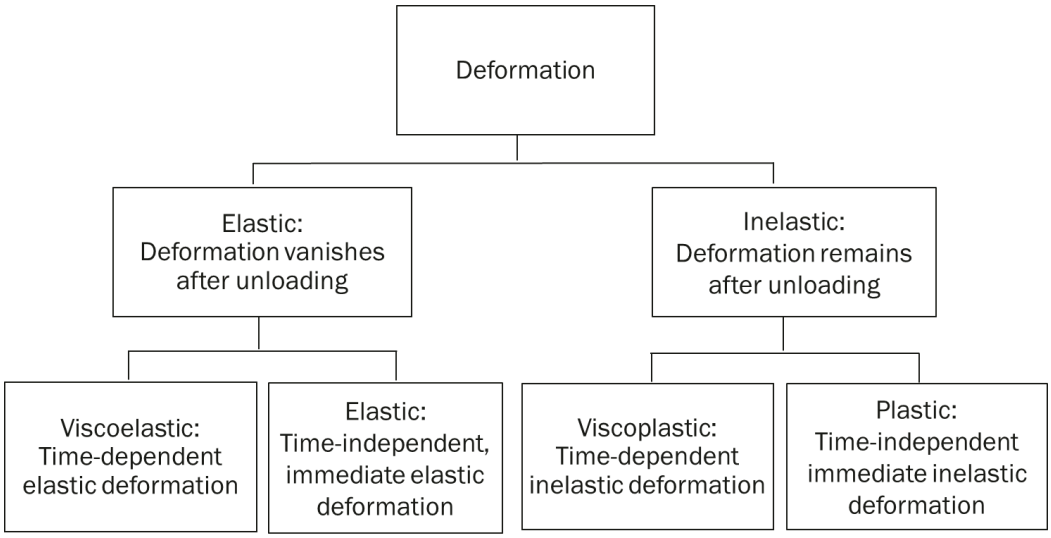

Figure 6. Classification of different types of deformation.

The different types of deformations often occur simultaneously. This is also the case with preloaded slip resistant connections where the viscoplastic creep deformation is accompanied elastic deformation and possibly also immediate plastic deformation. The total strain can therefore be written as the sum of elastic, plastic and creep components.

$$\varepsilon_{tot} = \varepsilon_e + \varepsilon_p + \varepsilon_c \qquad (7)$$

In computational approaches both inelastic deformation components are frequently considered as one single inelastic strain component ε_i.

$$\varepsilon_{tot} = \varepsilon_e + \varepsilon_i \tag{8}$$

Creep models based on decomposition (8) are called unified models. The two different ways of decomposing the total strain are illustrated in Figure 7.

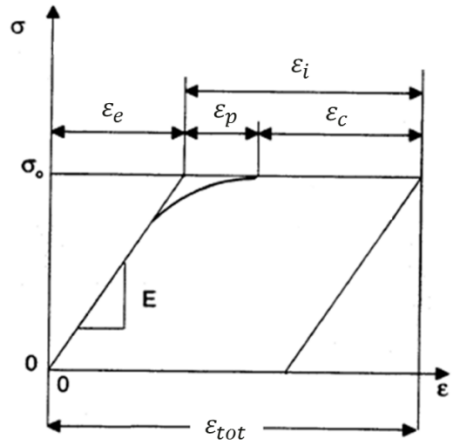

Figure 7. Decomposition of total strain in different components.

4. Creep theories

4.1. Classic creep theories

The first fundamental study on creep was published in 1910 by Costa Andrade [16]. This pioneering work initiated a systematic study of the phenomenon known as creep. The first generation of theories for creep deformation of metals, known as the classical creep theories, was developed in the following decades. The classical creep theories are analytical equations capable of describing the evolution of creep strain ε_c under instantaneously applied constant load σ at constant temperature T.

$$\varepsilon_c = \varepsilon_c(\sigma, t, T) \tag{9}$$

The influence of stress, loading time and temperature is typically factorized.

$$\varepsilon_c = f(\sigma)\, g(t)\, h(T) \tag{10}$$

A power law form is often used for the stress and time components

$$f(\sigma) \sim \left(\frac{\sigma}{\sigma_{ref}}\right)^n \quad \text{and} \quad g(t) \sim \left(\frac{t}{t_{ref}}\right)^m \tag{11}$$

where the values $0 < m < 1$ of the stress exponent correspond to primary creep and the value $m = 1$ corresponds to secondary creep. Other common forms for the stress function $f(\sigma)$ are given in Table 1.

The temperature dependency is often modelled with an Arrhenius type component

$$h(T) = e^{-\frac{Q}{RT}} \tag{12}$$

where Q denotes the activation energy for the underlying physical process and R is the gas constant [17].

Table 1. Common choices for the stress function in classic creep models [18] .

Stress function	Reference and year.
$f = A\left(\frac{\sigma}{\sigma_{ref}}\right)^n$	Norton, 1929
$f = A\left(\exp\left(\frac{\sigma}{\sigma_{ref}}\right) - 1\right)$	Soderberg, 1934
$f = A\sinh\left(\frac{\sigma}{\sigma_{ref}}\right)$	McVetty, 1936
$f = A\exp\left(\frac{\sigma}{\sigma_{ref}}\right)$	Dorn, 1955
$f = A\left\{\sinh\left(\frac{\sigma}{\sigma_{ref}}\right)\right\}^n$	Garofalo, 1965

In many applications, the load is neither constant nor applied instantly. In this case the creep law needs to be expressed in rate form

$$\dot{\varepsilon}_c = \dot{\varepsilon}_c(\sigma, t, T) \tag{13}$$

The rate form is obtained by differentiating the creep strain with respect to time. Creep rate laws in which time exists as independent variable are called *time-hardening* models. Elimination of time from equations (9) and (13) results in another formulation of the creep rate law.

$$\dot{\varepsilon}_c = \dot{\varepsilon}_c(\sigma, \varepsilon_c, T) \tag{14}$$

Creep rate laws in which creep strain exists as an independent variable are called *strain-hardening* models.

As an example we may consider the creep law resulting from the choices (11).

$$\varepsilon_c = A\left(\frac{\sigma}{\sigma_{ref}}\right)^n \left(\frac{t}{t_{ref}}\right)^m \tag{15}$$

This creep model is known as the Norton-Bailey or power law creep. The time hardening formulation of this creep law is given by

$$\dot{\varepsilon}_c = A\left(\frac{m}{t_{ref}}\right)\left(\frac{\sigma}{\sigma_{ref}}\right)^n \left(\frac{t}{t_{ref}}\right)^{m-1} \tag{16}$$

The corresponding strain hardening formulation is

$$\dot{\varepsilon}_c = A^{\frac{1}{m}} \left(\frac{m}{t_{ref}}\right) \left(\frac{\sigma}{\sigma_{ref}}\right)^{\frac{n}{m}} (\varepsilon_c)^{\frac{m-1}{m}} \quad (17)$$

Although the time hardening model (16) and the strain hardening model (17) will yield exactly the same response under instantaneously applied constant stress, they will yield different responses for gradually applied or varying loading.

In the literature on constitutive modelling [17,19] it is generally pointed out that the time hardening model can be used only for applications in which the loading is constant and applied instantaneously at a precisely known time $t = 0$. Therefore this form is not suitable for modelling preloaded bolted connections.

The transient creep at room temperature can be described by the following empirical logarithmic creep law for a large number of metals and alloys

$$\varepsilon_c = \alpha \ln t \quad (1)$$

where α is a creep parameter. The equation (1), however, predicts an infinite creep rate at $t = 0$. Therefore, as discussed by Oehlert at Atrens [20], this empirical model is commonly reformulated as

$$\varepsilon_c = \alpha \ln\left(1 + \frac{t}{t_0}\right) \quad (18)$$

for numerical calculations. The rate form of this creep law can be written as the a time hardening model as

$$\dot{\varepsilon}_c = \frac{\alpha}{t_0}\left(1 + \frac{t}{t_0}\right)^{-1} \quad (19)$$

or, alternatively, as a strain hardening model as

$$\dot{\varepsilon}_c = \frac{\alpha}{t_0} \exp\left(-\frac{\varepsilon_c}{\alpha}\right) \quad (20)$$

The creep parameter α in equations (1) - (20) is a function of stress. The stress dependency can be described e.g. by the functions summarized in Table 1.

4.2. Viscoplasticity with internal state variables

The second generation of creep models known as viscoplasticity with internal state variables started developing in the mid 1960's. In this approach, a number of internal state variables denoted here by β_i, are used to describe the evolution of the microstructure of the material. The creep rate $\dot{\varepsilon}_c$ is described as a function of observable variables (e.g. stress, creep strain and temperature) and internal state variables β_i.

$$\dot{\varepsilon}_c = \dot{\varepsilon}_c(\sigma, \varepsilon_c, T, \beta_i) \quad (21)$$

The creep constitutive law (21) must be complemented with evolution laws for the internal state variables.

$$\dot{\beta}_i = \dot{\beta}_i(\sigma, \varepsilon_c, T, \beta_i) \quad (22)$$

The constitutive equations (21) and (22) are frequently derived within the framework of continuum thermomechanics. This framework guarantees that the material behaviour is consistent with the second law of thermodynamics. [17,19,21,22]

The viscoplastic models with internal state variables are unified theories. The immediate and time dependent plastic deformations are treated as one inelastic strain component according to decomposition (8). The time-independent plasticity is obtained as a limiting case.

In low temperature applications dislocation glide is the dominating deformation mechanism as discussed the chapter 2. Therefore, the material behaviour is determined by the strength of different barriers to dislocation motion such as

A. interstitial and solute atoms,
B. grain boundaries,
C. precipitates,
D. density of mobile and sessile dislocations, and,
E. intergranular and intragranular residual stresses.

The hardening effects caused by solute atoms, grain boundaries and precipitates (A-C) do not evolve at room temperature. Therefore internal state variables are typically needed only for modelling the dislocation hardening and internal stresses in the microstructure. The number and type of internal state variables needed for describing these microstructural features varies widely depending on the specific application studied and on the desired level of complexity and accuracy of the model. The model of Hart [23,24] uses only one scalar state variable whereas the model proposed by Chaboche and Rousselier [25,25] has one scalar and two tensorial internal state variables, to name some examples.

5. Creep and stress relaxation testing

Creep deformation is normally studied either by creep tests or by stress relaxation tests. Both test methods have their advantages and disadvantages.

A creep test in its simples form involves subjecting a specimen to constant uniaxial stress state and measuring the elongation with time. Often the load is maintained constant. Constant load is a good approximation for constant stress provided that the creep strain is less than 1%. Traditional creep tests are relatively easy to conduct, and the results are easy to analyse. On the other hand, obtaining results for wide ranges of stress and strain rate is often time consuming and expensive since one test provides information only for a single stress level and since low strain rates can be usually achieved only after long testing periods. [1,2]

The alternative test method is called stress relaxation testing. A stress relaxation test typically involves loading a specimen to a desired extension under uniaxial stress state, and fixing the end points of the specimen at this position. As the specimen then continues to deform inelastically, the applied load relaxes according to the combined elastic compliance of the specimen and the load train [26,27].

The stiffness of servo-hydraulic testing machines is effectively infinite [27]. In this case the rate of creep deformation can be calculated from the rate of relaxation as follows

$$\dot{\varepsilon}_c = -\frac{\dot{\sigma}}{E} \qquad (23)$$

In contrast, electromechanical testing machines are usually fairly flexible. Neglecting the influence of machine compliance for this type of testing machine can therefore result in a gross underestimate of the plastic strain. Modern electromechanical testing machines are, however, often capable of keeping the total strain measured directly from the specimen at the specified constant value during the relaxation test. In this case, the flexibility of the machine becomes irrelevant and the equation (23) can be used for analysing the results.

The main advantage of stress relaxation testing is that a single stress relaxation test can often produce data over a wide range of strain rates. Consequently, obtaining results at low strain rates does not require as time intensive testing as with the traditional creep testing method. On the other hand, analysing the results of stress relaxation tests is more difficult than analysing the results of a creep test since in the relaxation tests both stress and strain rate are changing simultaneously. Stress relaxation tests also place high demands on the testing equipment; the load measuring device must be able to measure extremely small changes in the load as a function of time. [1,2,28]

6. Creep and stress relaxation of austenitic and ferritic stainless steels

6.1. Hart's phenomenological deformation theory

Professor E. W. Hart of Cornell University proposed in 1976 a theory for the non-elastic response of metals [23,24]. Hart's model is a state variable model. The material response is entirely determined by the current microstructure. The effect of prior plastic deformation is characterized by means of an evolutionary state variable σ^* which measures the strength of different barriers to dislocation motion. The inelastic response of the material is determined analytically through an equation of state

$$\dot{\varepsilon} = \dot{\varepsilon}(\sigma,\ \sigma^*, T) \qquad (24)$$

In Hart's model, inelastic deformation proceeds only as long as the stress exceeds the threshold determined by the state variable σ^*. The value of the internal state variable can therefore be identified as the saturation stress level which is approached asymptotically from above in a stress relaxation test. Consequently, stress relaxation tests were commonly used for determining the value of the state variable σ^* by Hart his co-workers.

The validity of Hart's model has been extensively studied. The model has been found to be in good agreement with the experimental results for wide variety of pure metals alloys under monotonic loading performed at slow strain rates [29–37]. Hart's model has been also successfully applied to austenitic stainless steels.

Yamada and Li carried out stress relaxation testing on AISI 304 and 316 type austenitic stainless steel at room temperature [33]. Their work was motivated by previous findings that low temperature stress relaxation curves of pure metals could be successfully described using Hart's state variable model. The purpose of Yamada and Li was to study if Hart's model can also applied to complex alloyed metals. Commercial AISI type 304 and 316 austenitic stainless steels were chosen as test materials since several different strengthening mechanisms such as precipitates, substitutional solutes, and interstitials are known to be active in these steels at room temperature. Yamada and Li found out that the behaviour of austenitic stainless steels follows a mechanical equation of state of the form

$$\dot{\varepsilon} = K(\sigma - \sigma^*)^m \qquad (25)$$

where *K* and *m* are material parameters. Figure 8 shows relaxation test results obtained for type 304 austenitic stainless steels. It can be seen that the state variable σ^* which determines the asymptotic stress level increases with increased loading in the relaxation test. Since the material follows the mechanical equation of state (25), relaxation curves obtained with different loads can be superposed into one single master curve as shown in the Figure 8(b).

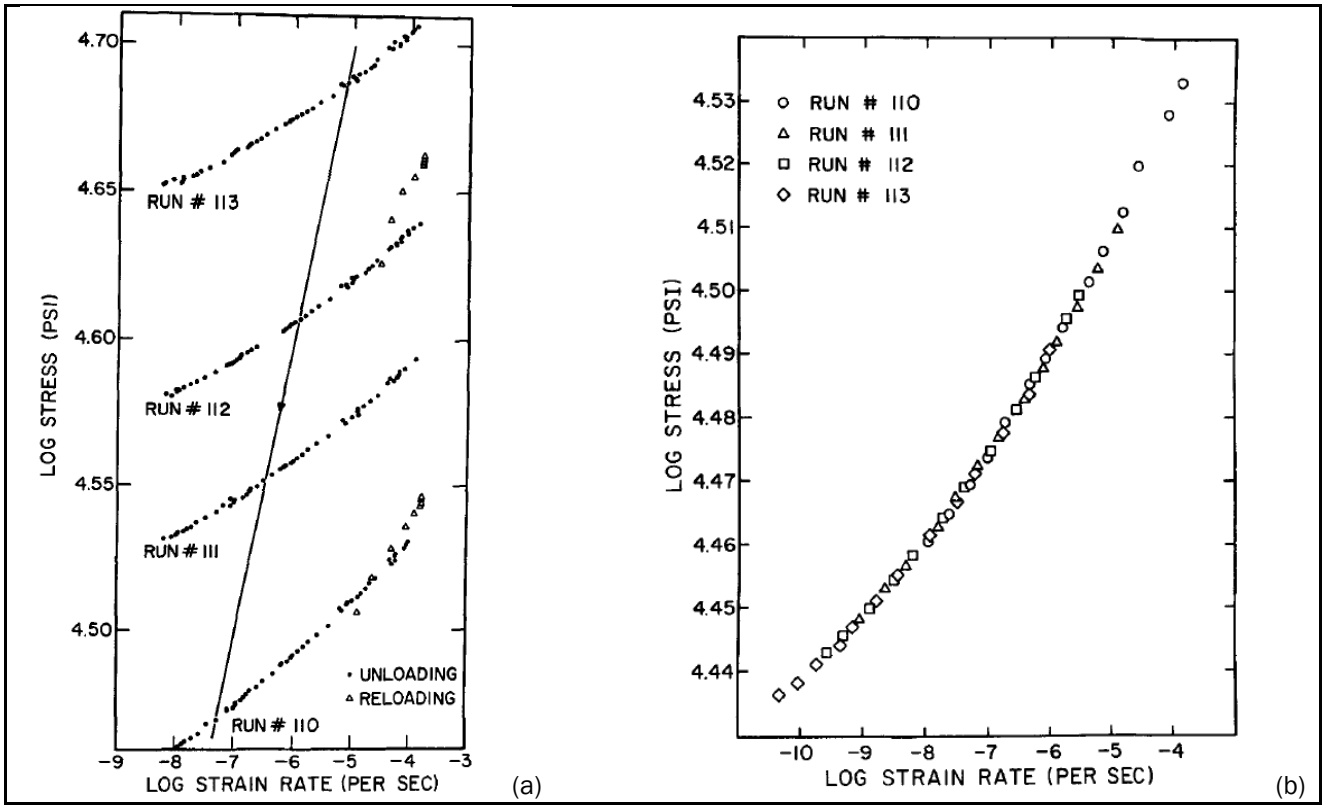

Figure 8. Relaxation test results for type 304 stainless steel [33]. (a) Measurement results for four different initial stress values. (b) Master curve constructed by superposing the other curves in (a) on the curve for run #110. The straight line in (a) depicts the scaling relation used for translating the curves.

The work on stainless steel was carried further by Hannula, Korhonen and Li [29]. They conducted a large number of stress relaxation tests on AISI 316 austenitic stainless steel at room temperature. It was found that the relaxation curves can be analytically described by the state equation

$$\dot{\varepsilon} = \dot{a}\left(\frac{\sigma-\sigma^*}{G}\right)^M \qquad (26)$$

where $\dot{a}(T)$ and the exponent M are material dependent constants. The value $M = 14.1 \pm 0.8$ was obtained for AISI type 316 austenitic stainless steel. The state variable σ^* determines the asymptotic lower bound for the stress relaxation. No stress relaxation or creep may occur below this stress level. As shown in Figures 9 and 10, the creep limit σ^* was approximately 80% of the load applied in the beginning of the relaxation run.

It worth noting that the loads applied by Hannula, Korhonen and Li were high enough to cause significant plastic deformation of the material. The total strain at the beginning of the relaxation test ranged from 0.3% to 29.5%.

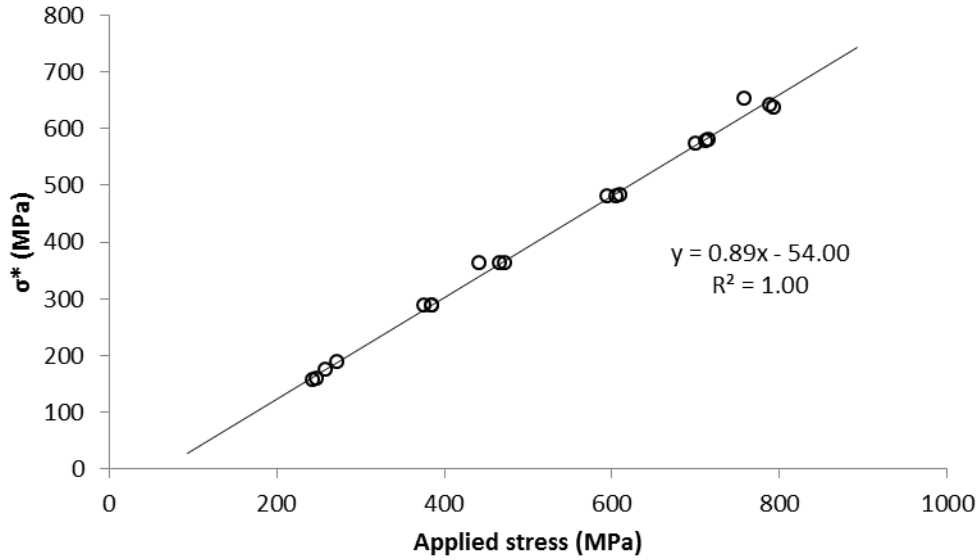

Figure 9. The relaxation limit was proportional to the applied loading.

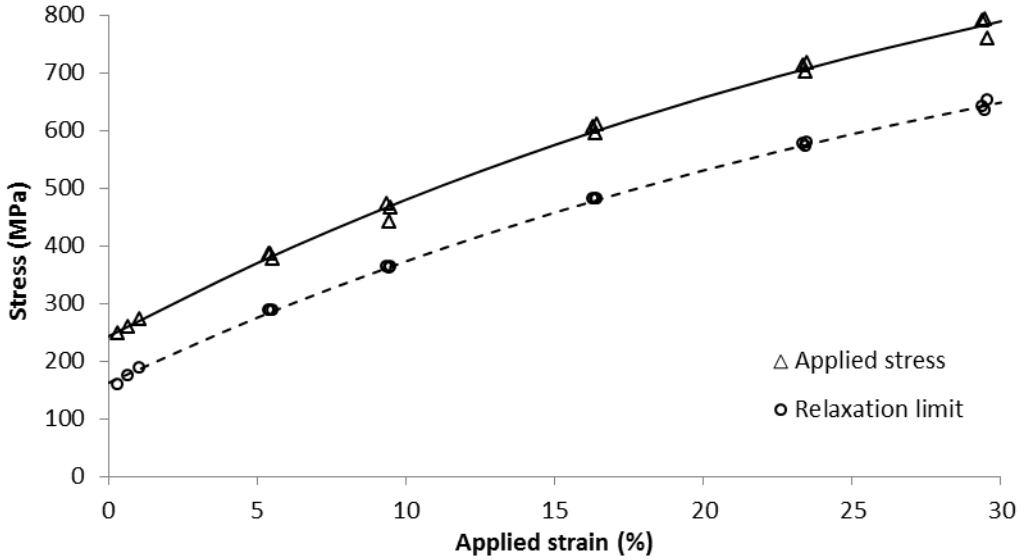

Figure 10. The applied load and the relaxation limit as a function of the strain applied in the beginning of the relaxation run along with polynomial fitting functions. The figure is based on the same test results as the Figure 9.

Hannula, Korhonen and Li [29] and Hannula and Li [30] also studied the behaviour of AISI type 316 austenitic stainless steel under repeated relaxation runs, Figure 11. They concluded that the material behaviour follows the same state equation (26) in repeated loadings. Furthermore, the asymptotic limit for the stress relaxation and the exponent *M* did not change between the repeats whereas the multiplier decreased. It follows that the stress was always relaxing towards the same asymptotic limit, but the speed at which this limit was approached decreased when the loading was repeated.

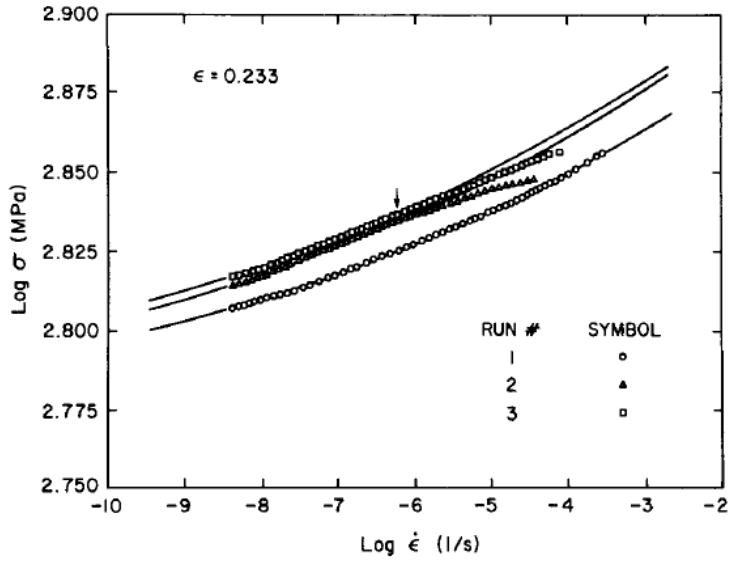

Figure 11. Stress-strain rate data from repeated relaxation runs on AISI type 316 austenitic stainless steel [29]. Above the point marked by the arrow, the delayed elastic (anelastic) deformation dominates the repeated relaxation behaviour. The state equation does not apply above this point in the repeats.

Hannula, Korhonen and Li summarize their findings on as follows [29]:

> *"It can be shown both theoretically and experimentally that the following relation holds during relaxation of 316 SS:*
>
> $$\ln \dot{\varepsilon} = \left(\frac{M}{1-M}\right) \ln(t+a) + C \qquad (27)$$
>
> *where M is the exponent [in equation (26) in this report] and C and a are constants. In 316 SS the time constant a is very small (order of 0.1 seconds), so for a good approximation it can be neglected."*

The creep law corresponding to (27) is given by

$$\dot{\varepsilon} = C'(t+a)^{\left(\frac{M}{1-M}\right)} \qquad (28)$$

where C' is another constant. The constant M in (28) equals to $M = 14$. Therefore, according to Hannula, Korhonen and Li, the creep deformation of AISI type 316 austenitic stainless steel follows the power law

$$\dot{\varepsilon} \sim t^{-1.08} \qquad (29)$$

Relaxation of type 316 austenitic stainless steel at elevated temperature was studied by Huang, Ellis and Li [36]. The authors carried out load relaxation experiments on type 316 stainless steel at different temperatures up to 650°C. At lower homologous temperatures ranging from 20°C to 200°C, the relaxation behaviour followed the plastic equation of state given by equation (26). The relaxation curves were concave upward. Above 200°C, the shape of the relaxation curves changed as shown in Figure 12. Therefore it was proposed that the deformation behaviour is controlled by two different physical processes. Dislocation glide controlled processes are important at lower homologous temperatures up to 200°C. Different diffusion controlled processes dominate above 500°C. And in the intermediate temperature range, between 200°C and 500°C, both mechanisms are influencing the material behaviour. Huang, Ellis and Li conclude that the equation of state (26) can be applied for AISI type 316 austenitic stainless steel up to 200°C. The relaxation behaviour of the material remains qualitatively similar throughout the range from room temperature to 200°C.

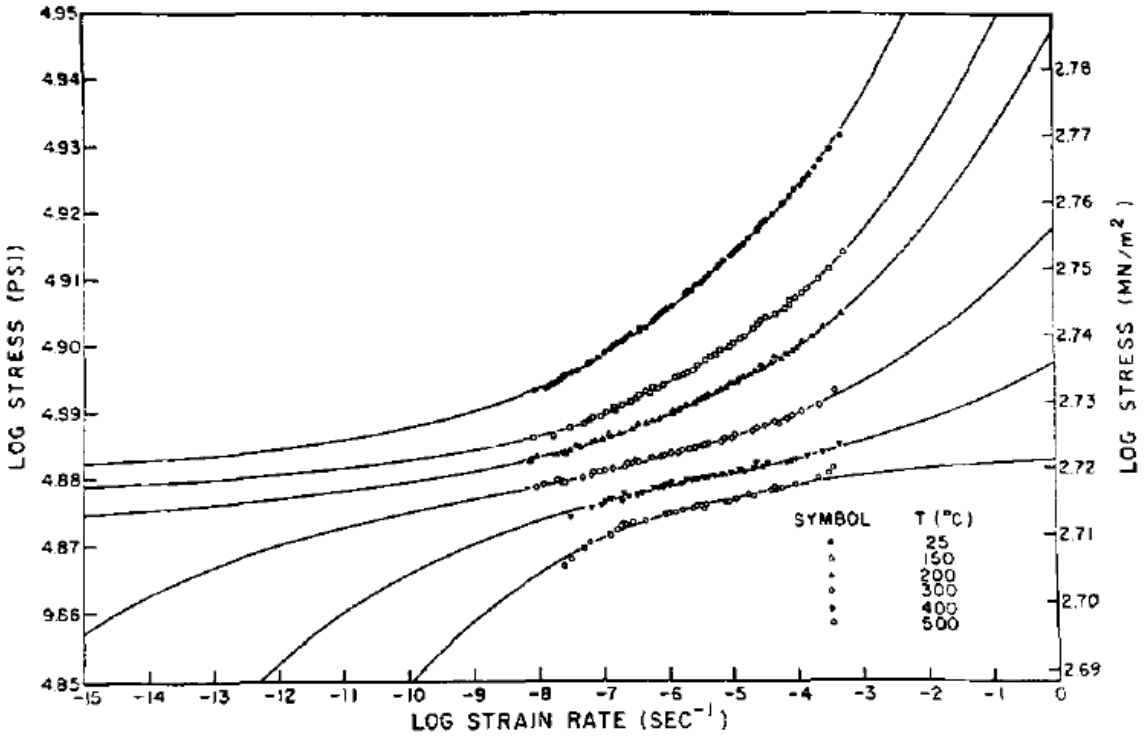

Figure 12. Relaxation curves measured for AISI type 316 austenitic stainless steel at different temperatures [36].

Stress relaxation of AISI type 316 austenitic stainless steel in solution-annealed state and in 20% cold-worked state was studied by Thomas and Yaggee [37]. The authors found that the stress relaxation response of both the solution annealed and the 20% cold worked material could be presented using the plastic equation of state proposed by Hart. It was also found that the relaxation curves of 20% cold worked material cannot be superposed to the same master curve as those of the solution annealed material, Figure 13.

The research conducted to within the framework of Hart's phenomenological deformation theory can be summarized as follows:

- The room temperature stress relaxation of austenitic stainless steel can be described using the plastic equation of state.

$$\dot{\varepsilon} = \dot{a}\left(\frac{\sigma-\sigma^*}{G}\right)^M \qquad (26)$$

  It follows that inelastic creep deformation proceeds only as long as the stress exceeds the threshold determined by the state variable σ*.
- The value of the state variable σ* characterizes the asymptotic lower bound for the stress in the relaxation experiments.
- The rate of creep deformation is a function of the overstress ($\sigma - \sigma^*$).
- The internal state variable σ^* increases when the material is plastically deformed.
- In one comprehensive test series [29], the relaxation limit was roughly 80% of the applied load.
- The state equation (26) appears to be valid also for cold-worked material and at elevated temperature ranging from room temperature to *T = 200°C*.

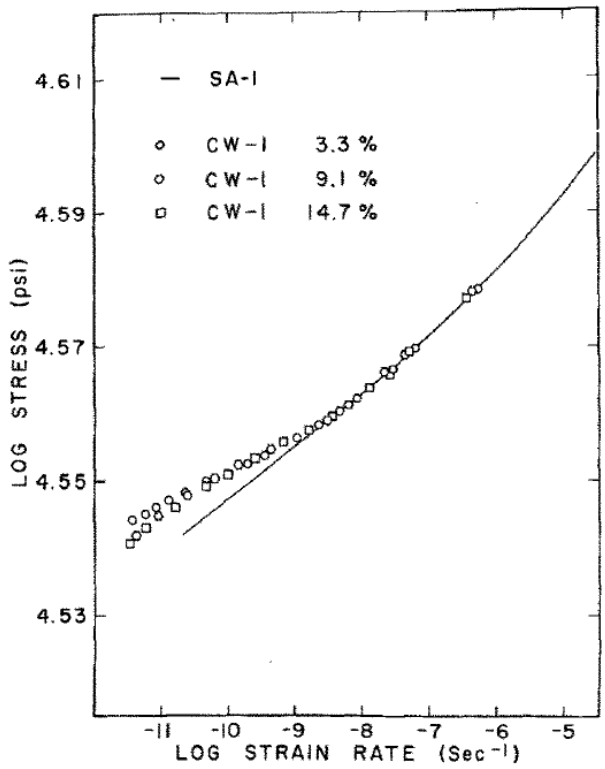

Figure 13. The relaxation curves of 20% cold worked material do not fit to the master curve obtained for the solution annealed material [37].

6.2. Krempl and co-workers

Krempl and his co-workers studied room temperature mechanical behaviour of AISI type 304 austenitic stainless steel in a series articles [38–41]. The material behaviour was studied in uniaxial tension using tensile tests, creep tests, relaxation tests and combinations thereof. The experimental results show considerable rate-sensitivity, creep and stress relaxation.

Figure 14 shows the results of three tensile tests measured with different strain rates. In two of the tests the strain rate was instantaneously changed by three orders of magnitude. The results show considerable rate sensitivity of the material in the plastic range. The fact that the stress-strain curves remain at constant distance from each other also suggest that the rate dependent part of stress is independent of plastic strain.

The authors also carried out combined relaxation and strain rate change tests in order to study the influence of strain rate and plastic strain on the relaxation behaviour. The results are shown in Figure 15. The results reveal several interesting features in the material response.

- The stress-strain curve always resumes the level corresponding to the current strain rate after each change of strain rate. There are no signs of any strain rate history effect.
- The stress drop during the relaxation period depends on the strain rate of the curve from which the relaxation commences.
- The stress drop during the relaxation period is independent of the plastic strain.

The last two observations receive further confirmation when the results of several similar stress-change and relaxation experiments are plotted as a function of the loading rate used between the relaxation periods, Figure 16. It can be observed that the test data can be completely explained by relaxation time and by the strain rate preceding the relaxation period. Therefore Krempl concludes that the change in stress in a given relaxation period does not depend on the actual value of stress and strain; the stress change depends only on the strain rate preceding the relaxation period.

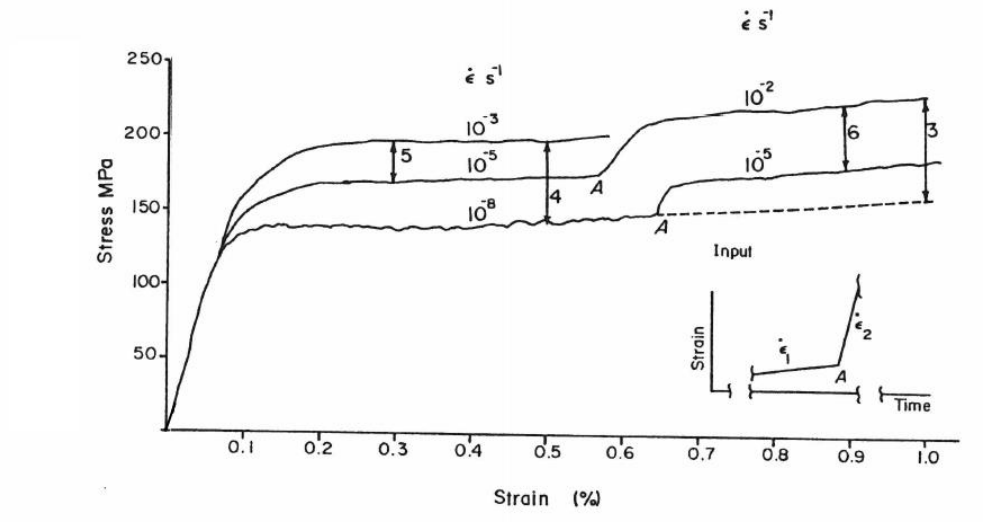

Figure 14. Stress-strain curves at for AISI type 304 austenitic stainless steel measured with different loading rates. The strain rate was instantaneously changed at points marked with A. Adapted from [38].

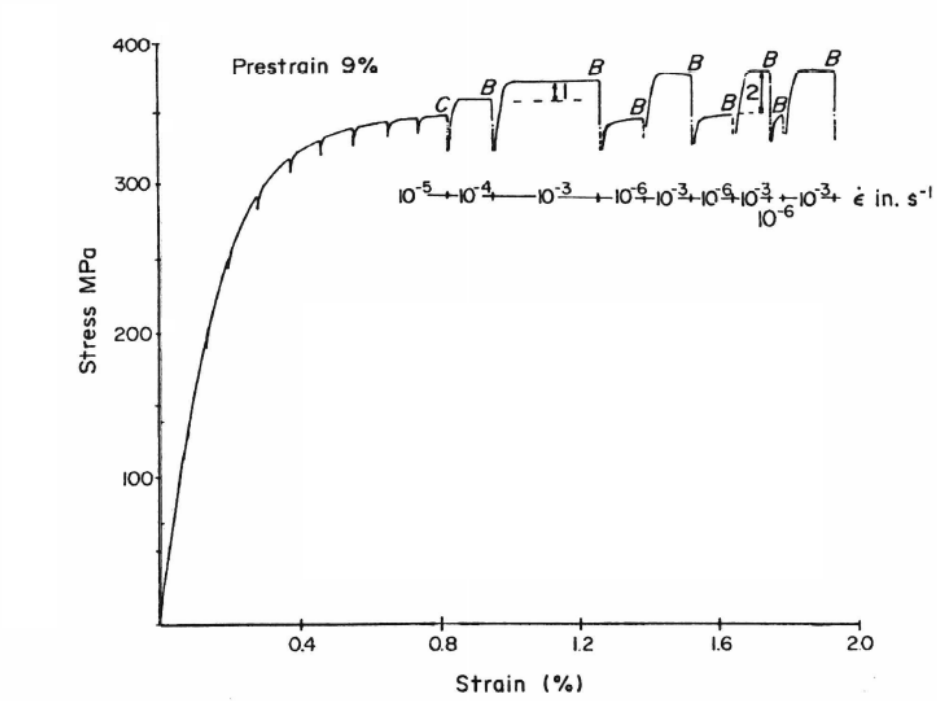

Figure 15. Relaxation and strain rate change tests. The strain rate used at different segments of the curve is indicated under the curve. At points marked with B, a relaxation test of 600 s is started. At strains below the point marked with C, the relaxation period is 30s. Adapted from [38].

The observation that the creep strain accumulated on in a given period of time depends strongly on loading rate preceding test was further studied by Kujawski, Kallianpur and Krempl [39]. Both creep and stress relaxation tests were used for investigating the phenomenon. The results confirm the previous findings, and they are summarized in Figures 17 and 18. Figure 17 shows creep test results for two specimens subjected to the same load. The loading rate of 6.9 MPa/s was used for specimen number II and 0.069 MPa/s for the other specimen. It can be seen that the rate of creep deformation is definitely higher for the specimen loaded with higher loading rate. Creep curves obtained for two different specimens subjected to different levels of stress with the same stress rate in loading phase are shown in Figure 18. Despite of the difference in loading, a single creep curve is obtained.

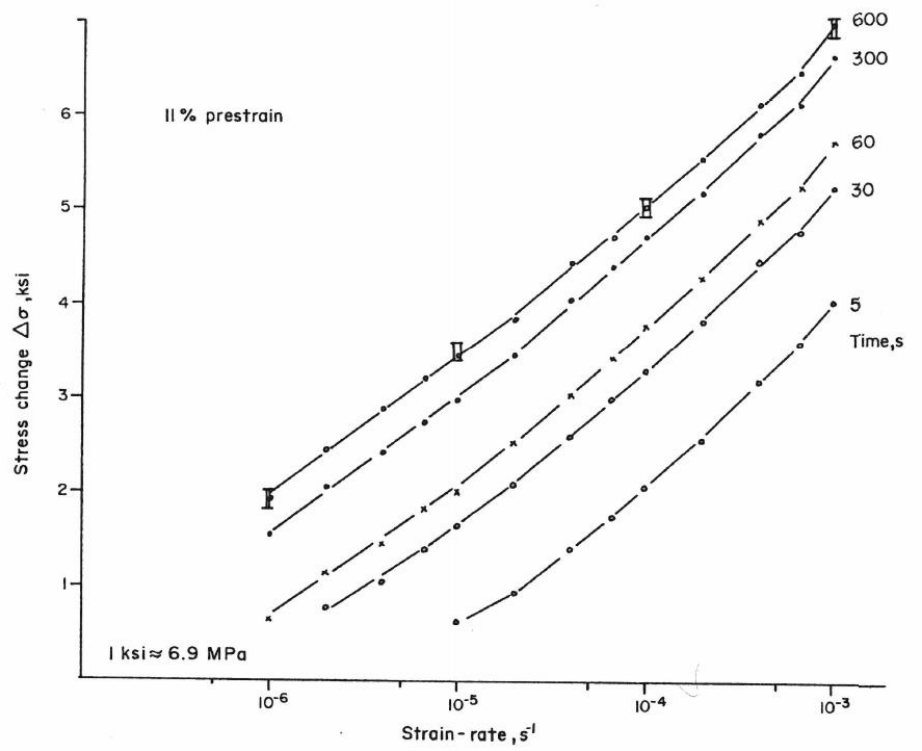

Figure 16. Stress change in relaxation test as a function of the strain rate before the relaxation run [38]. Points labelled by the Roman numeral II originate from Figure 15.

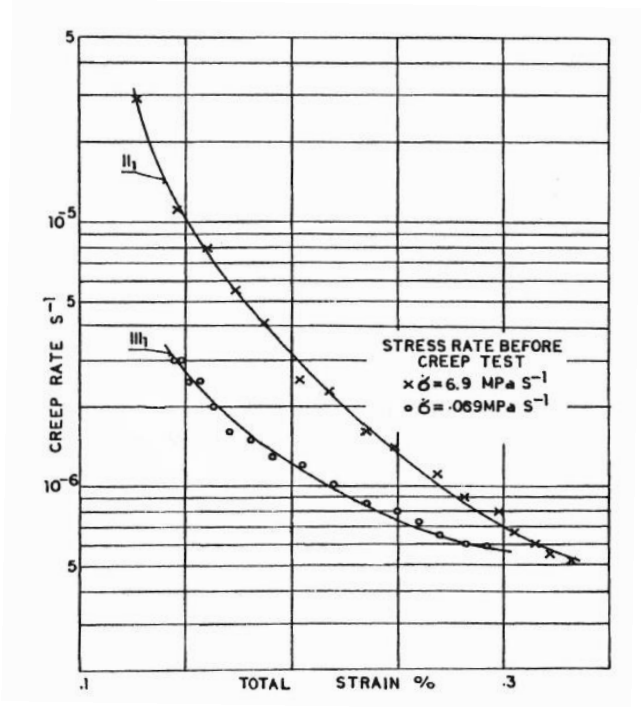

Figure 17. Creep rate for two specimens tested at the same stress level σ = 187 MPa. The loading prior to the creep test was carried out using widely different stress rates. Adapted from [39].

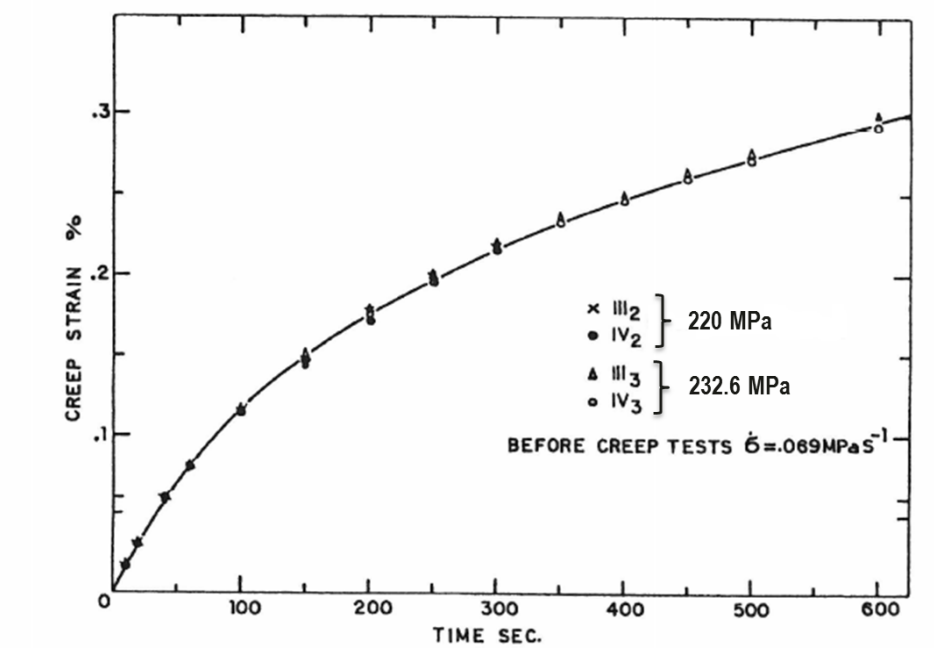

Figure 18. Creep curves for two different specimens subjected to different levels of stress with the same stress rate during loading. Adapted from[39].

Kujawski, Kallianpur and Krempl point out that a viscoplasticity theory based on overstress can explain the observed rate dependency and the gradual exhaustion of creep deformation during the creep period. The term viscoplasticity based on overstress refers to all theories in which the creep rate is described as a function of overstress between the current stress and a quasistatic (rate-independent) stress strain curve.

Further experimental studies on room temperature viscoplasticity of AISI type 304 austenitic stainless steel were conducted by Krempl and Kallianpur [40]. Multistep creep tests with a staircase loading were used to study the influence of loading history on the material behaviour. Figure 19 shows test results for one multistep creep test. When the load is increased between the creep steps, the curve joins the stress-strain curve measured in a tensile test conducted with the same constant stress rate which is used for increasing the load between the creep periods. It can be concluded that the material work hardens during the creep periods and that the work hardening caused by creep deformation equals to that caused by an equal amount of plastic strain in a tensile test.

The same authors also studied the influence of strain rate on the Bauschinger effect on AISI 304 type austenitic stainless steel. In the experimental test setup solid stainless steel cylinders were subjected to strain controlled loading and subsequent reverse loading in a servo-controlled tension-torsion testing machine. Different loading rates were used in the forward and reverse loading segments. Figure 20 shows test results obtained with this method. In the figure (a), two specimens were loaded using the same strain rate up to the maximum strain. Upon reversal the strain rates were changed. It was found that in this case the Bauschinger effect was more pronounced when slow strain rate was used in the reverse loading. In the figure (b), two specimens were loaded using different strain rates up to the maximum strain, and in this case, the same strain rate was used in the reverse loading. In the latter case, the Bauschinger effect was similar for both specimens. It can be concluded that the Bauschinger effect is independent of the loading rate used in the previous forward loading step. It depends only loading rate used in the reverse loading. These effects can also be reproduced by viscoplastic theories that are based on the overstress between the current stress and the rate-independent strength of the material.

6.3. Wu and Ho

Wu and Ho studied the strain hardening of annealed stainless steel by creep [42]. They conducted tension-torsion experiments on tubular specimens using a servo-hydraulic testing system. The equipment was used to determine the shape of the yield surface of the material before and after different loading sequences. It was found that transient creep causes the yield surface to undergo kinematic hardening with insignificant amount of isotropic hardening. The yield surface of material deformed by creep was compared with that deformed by monotonically increasing loading. It was concluded that the yield surface hardened by creep is the same as that hardened by plastic deformation. In spite of different deformation processes the material strain hardens by equal amount as long as the plastic strain is the same. The results corroborate the previous findings by Krempl and Kallianpur [40].

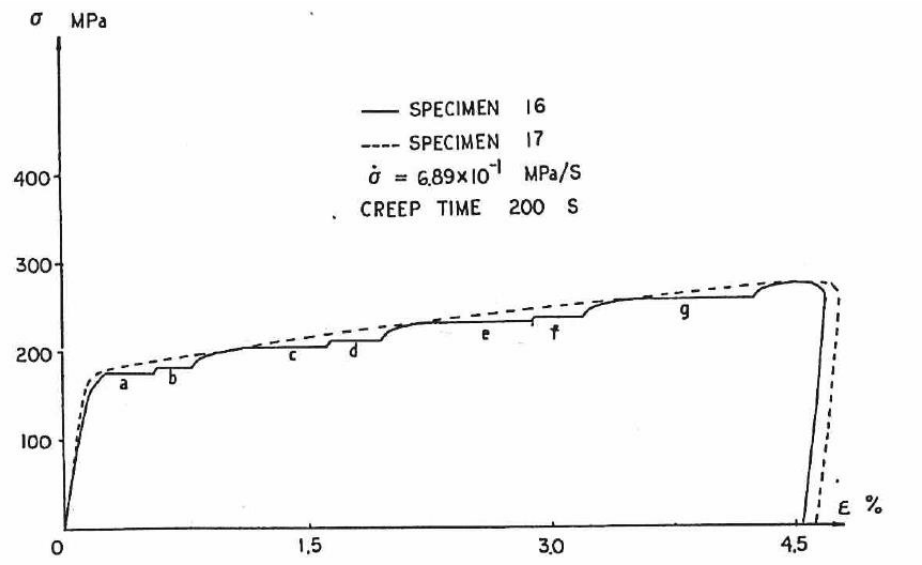

Figure 19. Multistep creep tests with staircase loading [40]. The loading is increased with a constant stress rate between the creep periods. The dashed curve shows the stress-strain curve for the constant stress rate used between creep steps

6.4. Alden

Alden studied tensile and creep deformation of AISI 304 type austenitic stainless steel at room temperature using a tensile testing machine [41]. He found that the creep strain depends strongly on the stress rate used in the loading phase in the beginning of the creep test. Figure 21 shows creep test results obtained for the same creep load with different loading rates. It can be observed that the creep strain is larger when the specimen is loaded to the creep stress at high stress rate. Figure 22 shows the rate of creep deformation for the same test. The initial creep strain rate strongly affected by the loading rate, but rapid decay brings the rate closer together after a few seconds. The findings confirm the earlier similar findings by Kujawski, Kallianpur and Krempl [39].

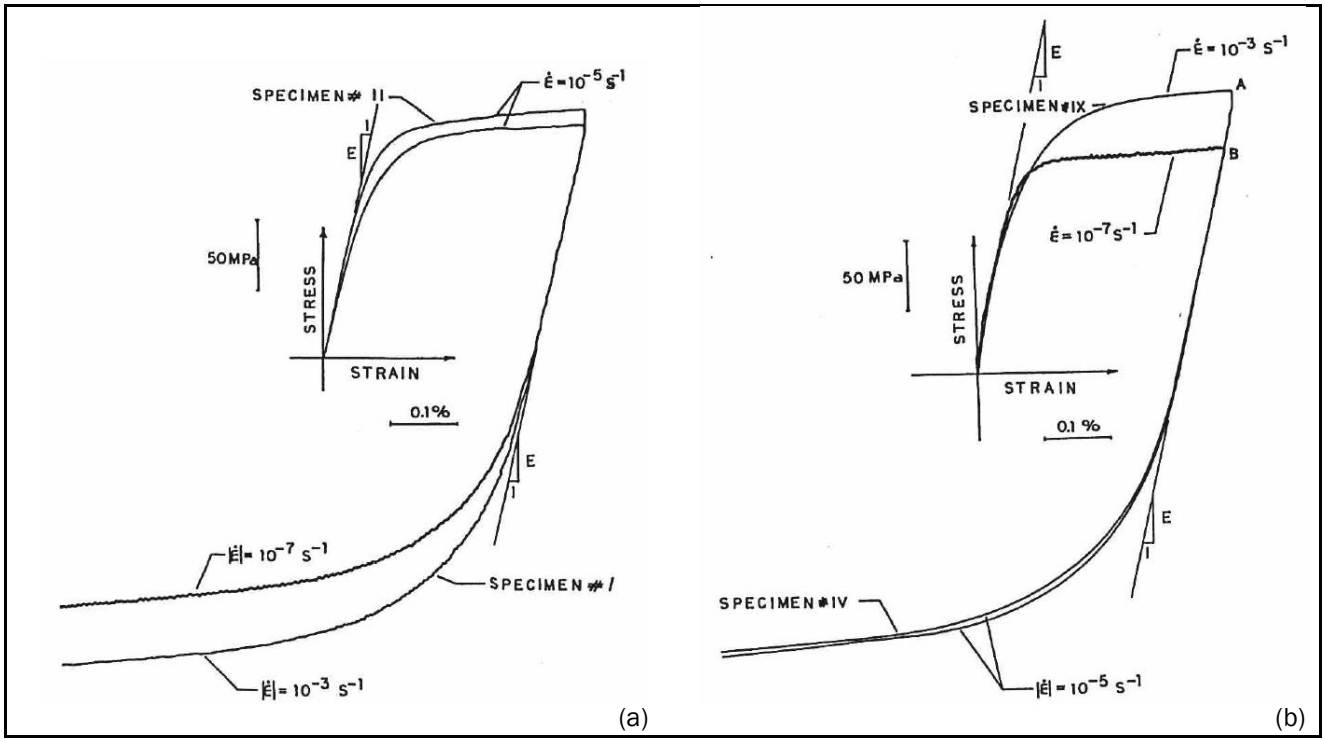

Figure 20. The effect of strain rate on the Bauschinger effect in AISI type 304 austenitic stainless steel [40].
(a) Same strain rate in forward loading, different strain rates in subsequent reverse loading.
(b) Different strain rates in forward loading, same strain rate in reverse loading.

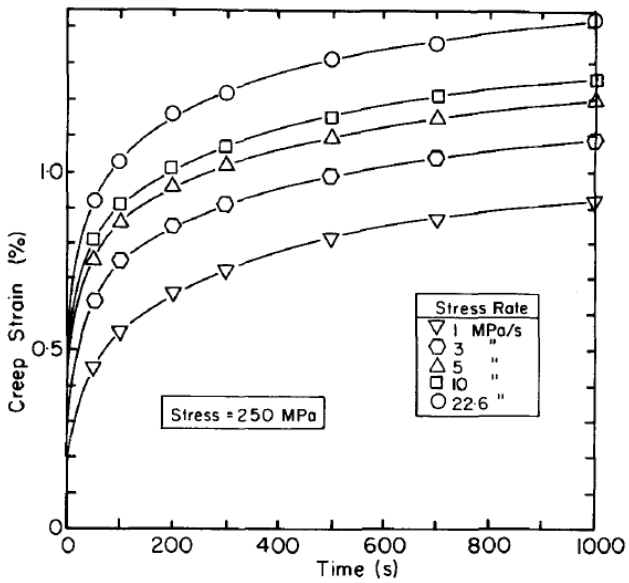

Figure 21. Creep strain increases as a function of the stress rate and time [41].

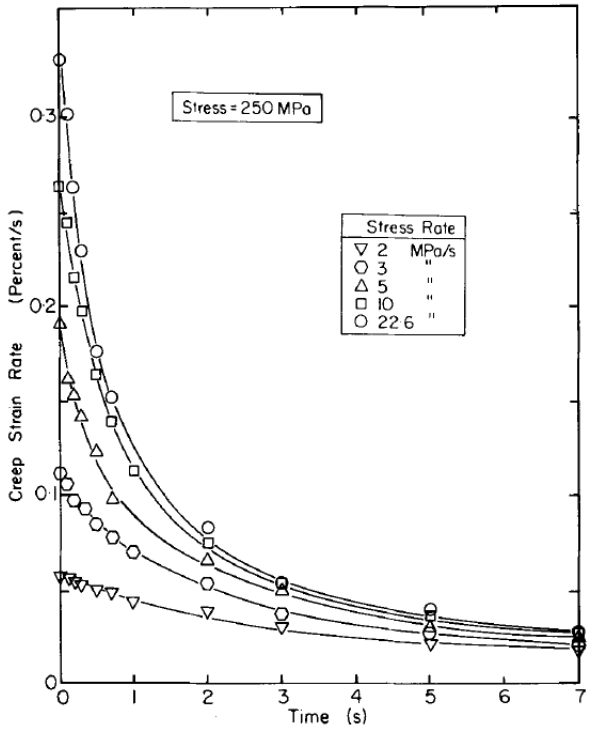

Figure 22. The creep strain rate as a function of time and loading rate [41].

6.5. Comparative studies by Schmidt and von den Steinen

Schmidt and von den Steinen made comparative studies [43–45] on the room temperature creep characteristics of steels with different crystal structures and different microstructures. Their test materials included common structural steel, quenched and tempered steel, martensitic steel, austenitic stainless steels and ferritic stainless steels. The authors concluded that there are no fundamental differences in the room temperature creep behaviour of materials with different crystal structure. Test materials with martensitic (BCT), ferritic (BCC) and austenitic (FCC) crystal structure behaved in a qualitatively similar manner in the room temperature creep tests. It is concluded that other factors characterizing the microstructure affect creep behaviour more strongly than the crystal structure.

Figure 23 shows measured creep test curves for type 1.4510 ferritic stainless steel and for type 1.4401 austenitic stainless steel. No fundamental differences can be observed in the room temperature creep characteristics of these two grades. Both grades deformed in fairly similar manner. The amount of plastic strain obtained after roughly 300 hours of sustained creep loading is also of the same order of magnitude for these two materials. Schmidt and von den Steinen [43–45] report similar test results for several different stainless steel grades.

Based on extensive experimental studies Schmidt and von den Steinen finally conclude that the creep behaviour is controlled by two characteristic values named the creep limit and the creep resistance. Both variables are related to the tensile stress-strain behaviour of the material. The creep limit determines the upper limit for purely elastic behaviour. No creep or stress relaxation may occur below this stress level. For practical purposes it can be assumed that the creep limit equals to the 0.01% proof strength of the material. The creep resistance defines how the creep deformation decelerates. The creep resistance is determined by the hardening exponent *n* describing the slope of the true stress vs. logarithmic plastic strain curve. A rapid work hardening results of rapid deceleration of the creep deformation. [43]

Schmidt and von den Steinen also concluded that the creep characteristics of different types of steels can be determined by short term testing. The creep deformations after 166 hours tests were proportional to those obtained after 15 minutes of sustained loading. [45]

According to Schmidt and von den Steinen [43–45] the existence of a sharp yield point plays in important role in the room temperature creep behaviour. Materials with a sharp yield point showed very little creep deformation below the lower yield stress R_{eL} and significant transient creep deformation above this limit.

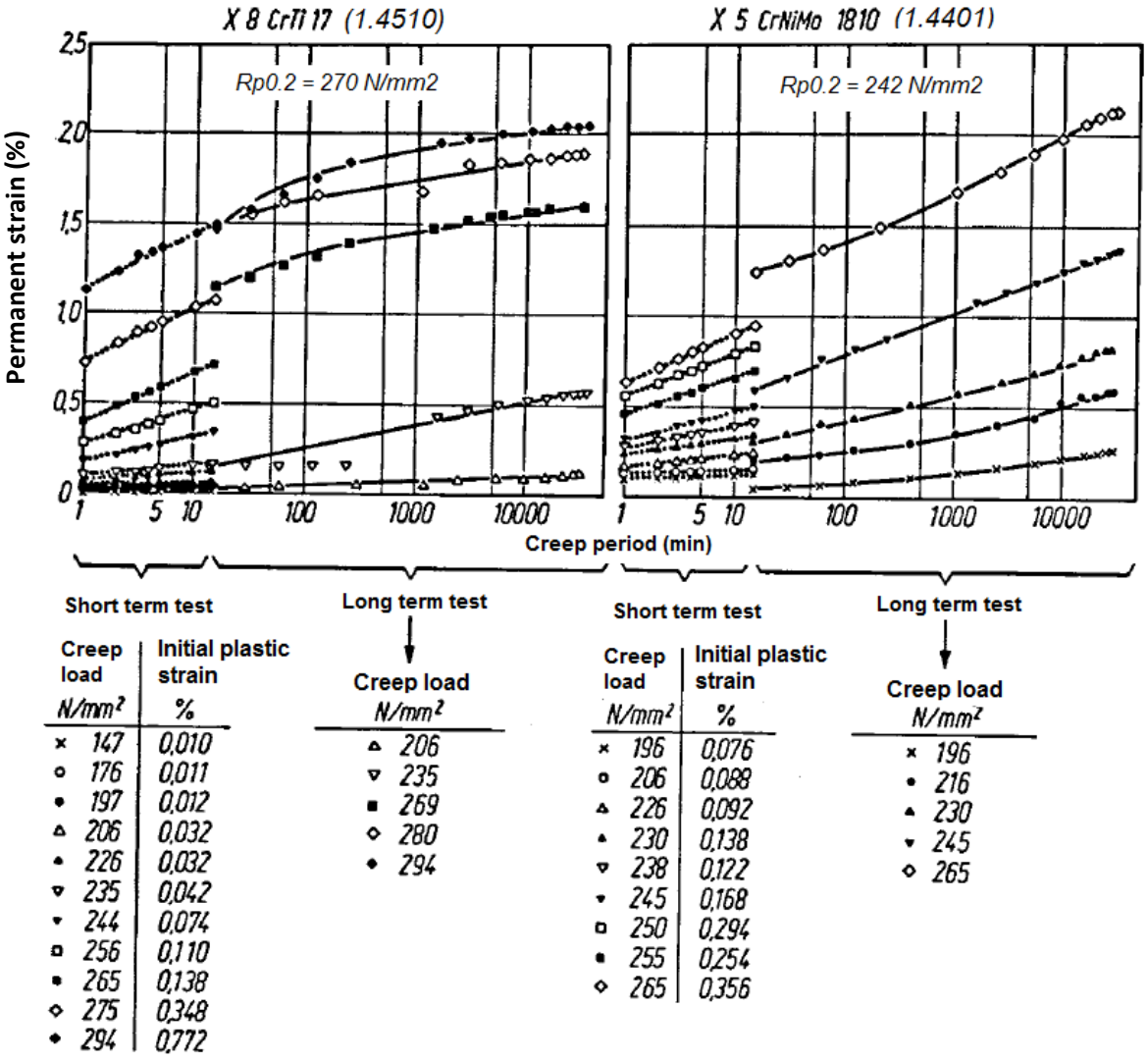

Figure 23. Room temperature creep test results for stabilized ferritic stainless steel 1.4510 and Mo-alloyed austenitic stainless steel 1.4401. Adapted from [44].

6.6. Schmidt and Dietrich

The research work of Schmid and von den Steinen was continued by Schmidt and Dietrich [46]. They carried out short term and long term creep tests on austenitic and ferritic stainless steels using various loading levels in order to study further the room temperature creep behaviour of stainless steels.

Figures 24, 25 and 26 show constant load creep test results for type 1.4401 austenitic stainless steel and type 1.4510 and 1.4016 ferritic stainless steels. The mechanical properties of these steels are summarized in Table 2. The type 1.4016 ferritic stainless steel had a sharp yield point whereas the other two showed smooth, gradual yielding. In the long term creep tests all three grades deformed in similar manner. The amount of plastic strain obtained after roughly 300 hours of sustained creep loading was also of the same order of magnitude for all three materials. In the short term (*15 min*) creep tests, there was however a notable difference between the grades. The difference is related to the existence of a sharp yield point and can be described as follows:

- The creep curves measured for grades 1.4401 and 1.4510 with smooth yielding were always smooth and concave irrespective of creep load and time period.
- The creep curves measured for the grade 1.4016 were also smooth and concave provided that the creep load was above the upper yield strength R_{eH} of the material.
- If the creep load for the grade 1.4016 was lower than the upper yield strength R_{eH}, the rate of creep deformation was extremely slow in beginning of the creep test. Later on, after reaching a certain threshold creep strain, the creep rate increased abruptly.

Therefore, there were two distinct phases in the creep deformation of the grade with sharp yield point. The shape of creep curves was quite different from those measured for the other grades.

The main research topic of Schmidt and Dietrich [46] was the influence of prior plastic deformation on the creep limit and creep resistance. These two materials characteristics had been earlier introduced by Schmidt and von den Steinen [43]. The former value determines the threshold stress needed for the inelastic creep deformation to proceed. The latter defines how quickly the creep deformation decelerates.

The testing procedure employed by Schmidt and Dietrich consisted of two distinct phases. In phase one the test material was pre-strained in uniaxial tension to different plastic strains in the range from 0% to 1.0%. In phase two, constant load creep tests were carried out under uniaxial tension or compression. The stress strain behaviour of pre-strained material was also studied by means of uniaxial tension and compression tests. The test material was grade austenitic stainless steel of grade 1.3974.

The tension and compression tests showed, as expected, that prior cold work may either increase or decrease the elastic limit depending on the direction of the second loading. In forward reloading, the elastic limit was increased whereas in reverse reloading it was decreased, Figure 27. This phenomenon is known as the Bauschinger effect and was first observed already in 1886 by German Engineer Johann Bauschinger [42].

The results concerning the creep limit and creep resistance were opposite to those obtained for monotonically increasing loading. The creep limit and the creep resistance increased in reverse reloading and decreased in forward reloading, Figure 28. Therefore it was concluded that the elastic limit stress is less important for the creep resistance than the rate of strain hardening; the steeper slope of the curve for the tension-compression case in the Figure 27 is associated with a high creep resistance and rapid deceleration of the creep process.

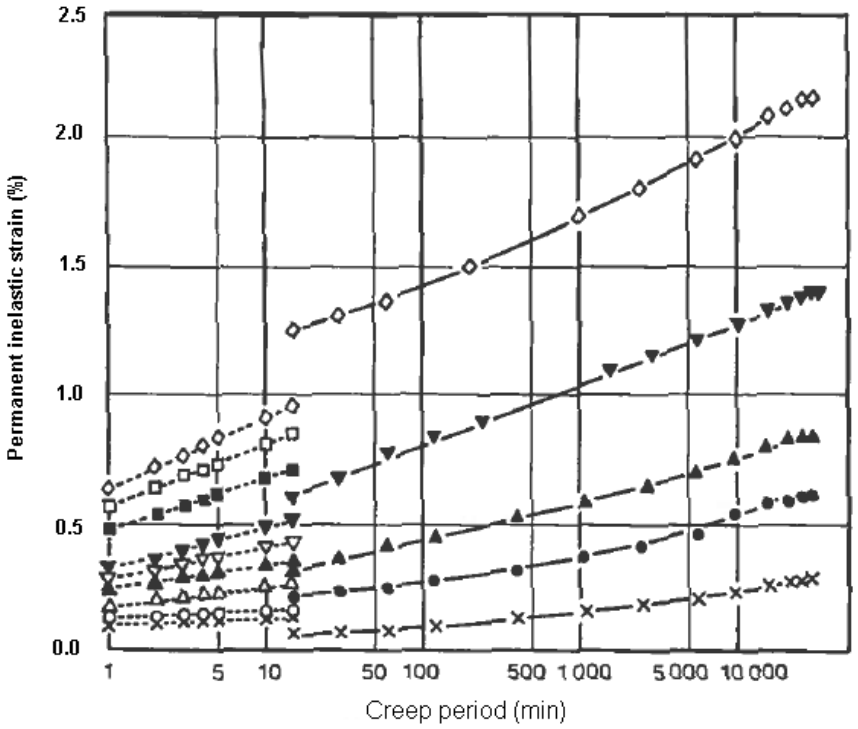

Short term test		Long term test
Load (MPa)	Initial plastic strain	Load (MPa)
196	0,076	196
206	0,088	216
226	0,029	230
230	0,138	245
238	0,122	265
245	0,168	
250	0,294	
255	0,254	
265	0,356	

Figure 24. Permanent inelastic deformation in short term and long term constant load creep tests of type 1.4401 austenitic stainless steel. The 0.2% proof strength of the material was 242 MPa. Adapted from [46].

Table 2. Mechanical properties of stainless steels studied by Schmidt and Dietrich [46].

Grade	Type	ReH (MPa)	ReL (MPa)	Rp0.2 (MPa)	Rm (MPa)	A5 (%)	Sharp Yield Point
1.4401	Austenitic	-	-	242	573	54	No
1.4016	Ferritic	301	294	-	497	28	Yes
1.4510	Ferritic	-	-	270	474	34	No

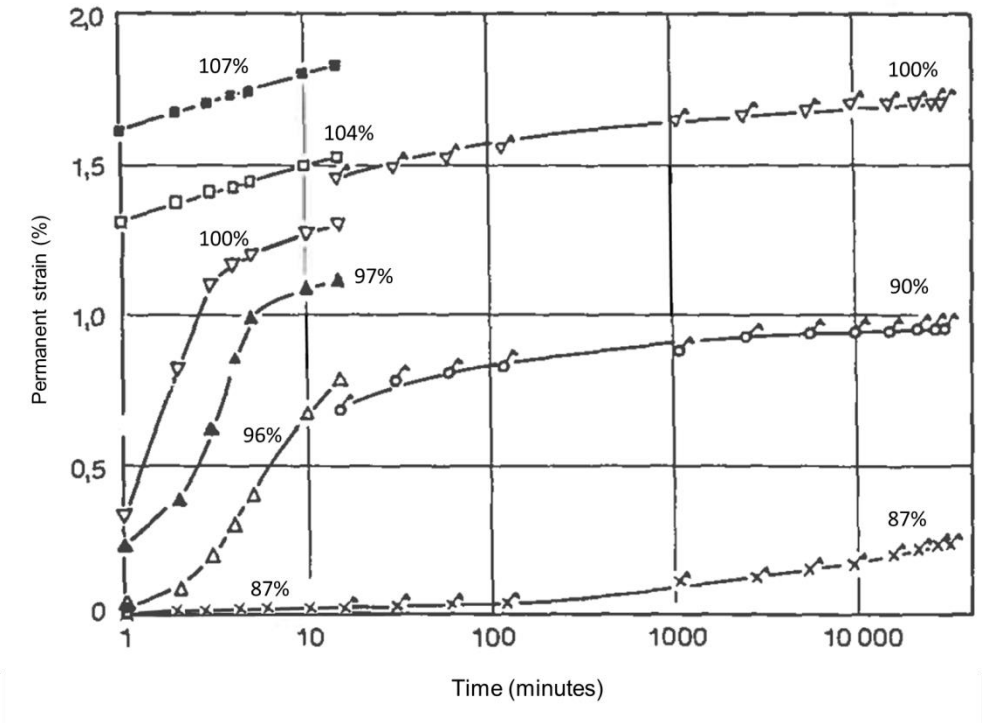

Figure 25. Short term and long term creep tests results for grade 1.4016 ferritic stainless steel. The test material had upper and lower yield point. The creep load ($\frac{\sigma}{R_{eL}}$) is given as curve parameter. Modified from [46].

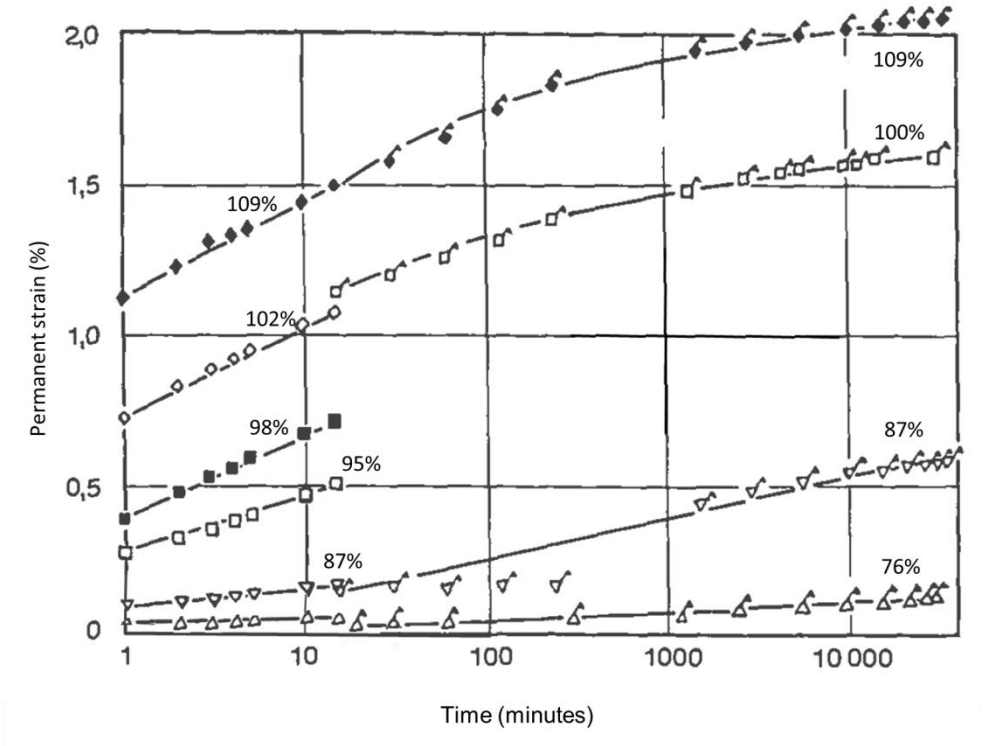

Figure 26. Short term and long term creep tests results for grade 1.4510 ferritic stainless steel. The test material showed smooth yielding. The creep load $\left(\frac{\sigma}{R_{p0.2}}\right)$ is given as curve parameter. Modified from [46].

Schmidt and Dietrich also studied the influence of mild heat treatments on the Bauschinger effect. The test material was again grade 1.3974 austenitic stainless steel. They found that a short heat treatment at a relatively low temperature in the range from 300°C to 500°C can be used to improve the elastic limit in reverse reloading. The increased strength did not, however, cause notable improvement in the creep characteristics. This led the authors to conclude that the Bauschinger effect in creep is different from that in monotonically increasing loading.

It is worth noting that the pre-strains induced in the material by Schmidt and Dietrich [46] in the preloading phase were small. Therefore their conclusions do not apply for heavily cold worked material such as temper rolled (2H) materials. Another detail worth noting is that the heat treatments applied did not cause a sharp yield point to emerge in the stress-strain curve. As discussed above, the existence of a sharp yield point may have a strong effect on the room temperature creep behaviour.

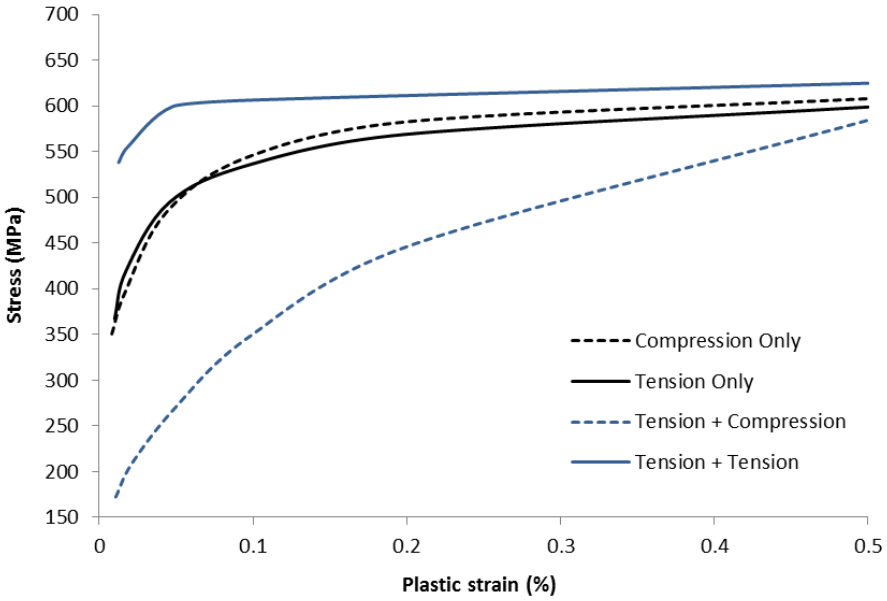

Figure 27. Stress-strain curves for material preloaded in tension by 0.5% before being subjected to tension or compression testing. Tension and compression test results for the virgin material are shown for reference. The tested material was grade 1.3974 austenitic stainless steel. Based on results by Schmidt and Dietrich [46].

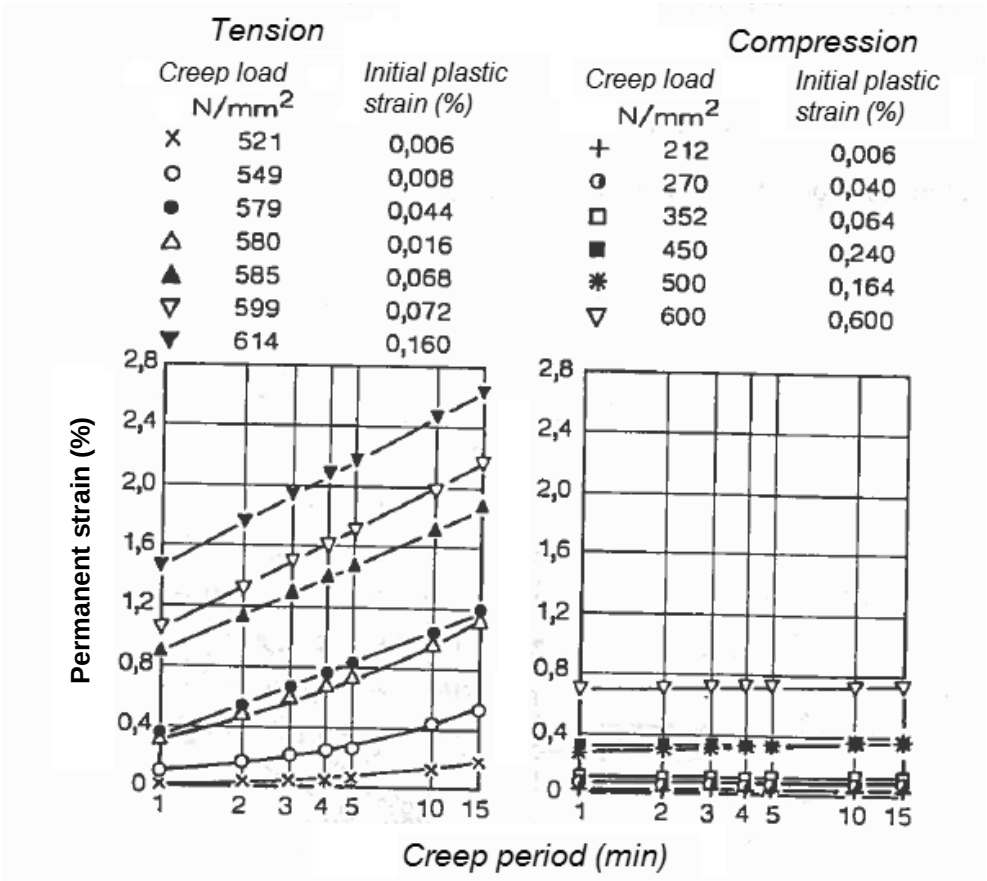

Figure 28. Creep curves measured under tensile and compressive loading for material subjected to 0.5% pre-strain in tension. Adapted from [46] .

6.7. Tendo, Takeshita, Nakazawa and Abo

Tendo, Takeshita, Nakazawa and Abo [47] studied the room temperature creep behaviour of austenitic stainless steels strengthened by different methods. Their test materials included altogether eleven austenitic stainless steels with varying chemical composition and strength. The strength increase was brought about by nitrogen alloying, cold rolling or precipitation hardening. Five experimental melts based on high purity 18%Cr - 14%Ni steel were used to examine the influence of carbon and nitrogen alloying. Common structural steel and interstitial free low carbon steel were used as reference materials. The properties of all studied materials are summarized in Table 3.

Figure 29 shows the creep strain in a constant load creep tests for SUS type 304 austenitic stainless steel in solution annealed condition and for common structural steel SM41. In the case of the structural steel, no creep deformation was observed over the period of 1000 hours after the initial strain caused by the loading. The austenitic stainless steel on the other hand showed transient creep with continuously decreasing creep rate.

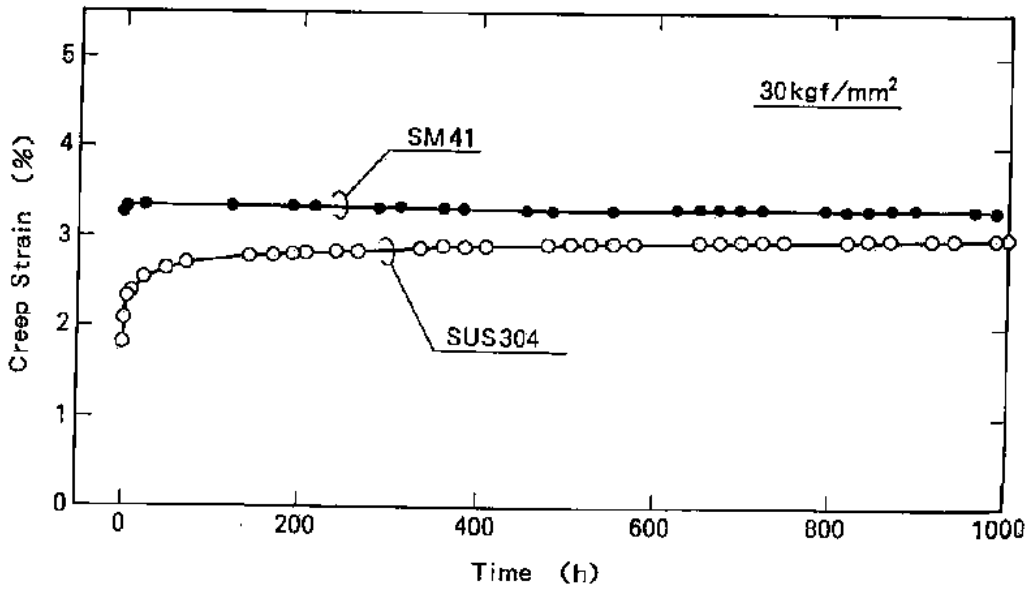

Figure 29. Room temperature creep curves for SUS 304 and common structural steel SM41 [47].

Figure 30 shows the creep strain cumulated after the first hour in a 1000-hour constant load creep test for materials strengthened with different hardening methods. In Figure 30(a), the creep strain is presented as a function of load level for solution annealed materials with different levels of nitrogen alloying. The 0.2% proof stress values were 270, 402 and 447 MPa for these three materials. Two features can be observed in the curves:

- The creep curves have a sharp corner located approximately at the 0.2% proof stress.
- The creep strain curves shift to higher stress according to the 0.2% proof stress values.

Figure 30(b) shows similar test results for materials work hardened by cold rolling. The curves are again shifted to the right corresponding to their 0.2% proof stress values. In contrast to the solution hardened materials, the curves measured for cold worked materials do not possess a sharp corner in the vicinity of the measured 0.2% proof stress value. The precipitation hardened material N280 showed little creep deformation below the 0.2% proof stress, but the creep strain increased very rapidly when the 0.2% proof stress was reached, Figure 30(c).

The effect of hardening mechanism on the room temperature creep behaviour of austenitic stainless steels is summarized in Figure 31. It can be seen that the hardening mechanism plays a role in the creep behaviour. If the creep resistance were determined only by the 0.2% proof strength of the material, all curves shown in Figure 31 would coincide. In the present case, however, the creep elongation varies with the hardening mechanism used to strengthen the material. From the creep resistance point of view, nitrogen alloying is the least effective way of strengthening material. The creep resistance of cold worked SUS 304 material is slightly better than that of the same material in solution annealed state. The precipitation hardened grade N280 showed very little creep elongation below the 0.2% proof stress and even above this limit the creep elongation was smaller than that of the other materials.

The effect of carbon and nitrogen alloying on room temperature creep behaviour is different even though both elements can be used for solid solution hardening of austenitic stainless steels, Figure 32. The nitrogen strengthened materials showed higher creep strain than those strengthened by carbon. The authors suggest that the difference is caused by decrease in the stacking fault energy caused by nitrogen. Transmission electron microscopic studies revealed well defined planar dislocation structures in the nitrogen alloyed samples whereas the dislocation structures were of entangled type in the other cases.

Table 3. Chemical composition, condition and 0.2% proof stress of materials studied by Tendo et al. [47]. Different conditions are denoted as follows: SA = solution annealed, CR = hardened by cold rolling, PH = precipitation hardened.

Material	Chemical composition (wt-%)							$R_{p0.2}$ (MPa)	Condition
	C	Si	Mn	Ni	Cr	N	Others		
SUS 304	0.056	0.6	0.9	9.2	18.9	0.03		270	SA
								498	CR 10%
								680	CR 20%
SUS 304N2	0.053	0.8	1	8	18.7	0.171	Nb: 0.1	402	SA
YUS 170	0.032	1.1	0.5	13	24.1	0.394	Mo: 0.7	447	SA
N280	0.007	0.3	0.8	33.7	18.5	0.002	Ti:2.0, Al:0.6	661	PH
A	0.02	< 0.1	< 0.1	14.5	17.9	0.001		157	SA
B	0.055	< 0.1	< 0.1	14.4	17.6	0.001		180	SA
C	0.112	< 0.1	< 0.1	14.8	18.1	0.001		221	SA
D	0.003	< 0.1	< 0.1	14.6	18.1	0.05		183	SA
E	0.003	< 0.1	< 0.1	14.7	18.3	0.128		227	SA
SM41	0.173	0.2	0.7			0.002		R_{eH} = 257	
TI-SULC	0.002	0.02	0.11			0.001	Ti: 0.06	88	

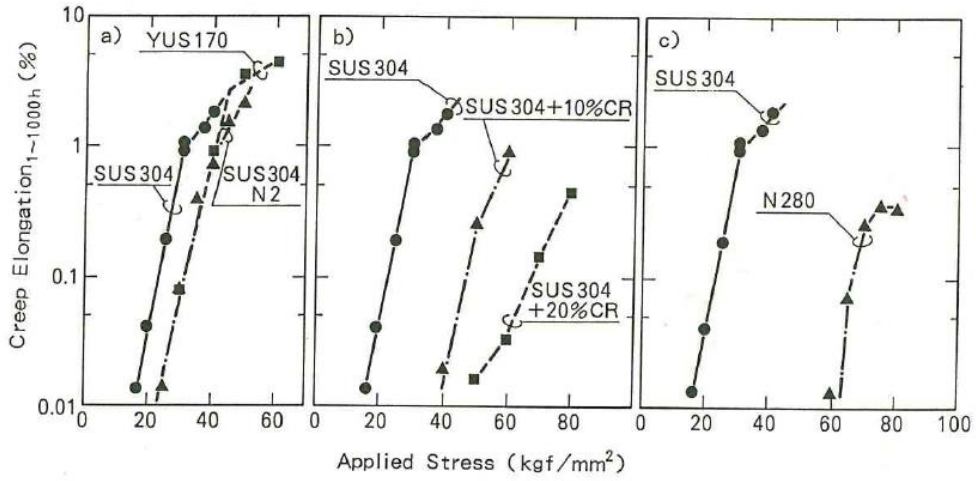

Figure 30. Creep strain from 1 hour to 1000 hour as a function of loading for different types of materials [47].
a) Solution annealed materials with different nitrogen levels.
b) Solution annealed and cold worked material.
c) Precipitation hardened material.

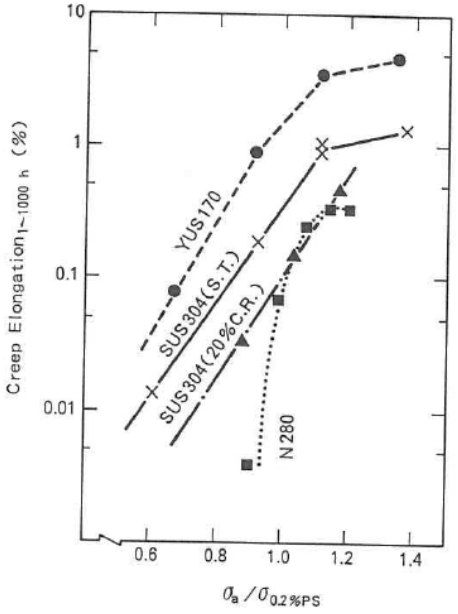

Figure 31. Relation between normalized stress and creep elongation [47].

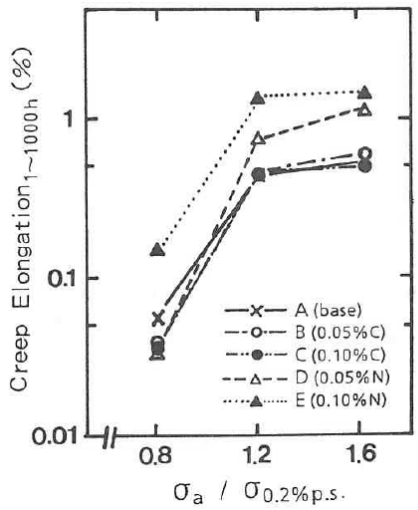

Figure 32. Relation between creep elongation and normalized stress for materials A-E with different amounts of carbon and nitrogen in solid solution [47].

Tendo, Takeshita, Nakazawa and Abo [47] also conducted creep tests on interstitial-free low carbon steel and found that this type of carbon steel shows similar transient creep as the austenitic stainless steels they studied. The main difference between the interstitial-free steel and the common structural steel is that in the former material the interstitial carbon and nitrogen atoms are removed from the solid solution. Therefore it was concluded that interaction of dislocations with interstitial atoms plays an important role in the room temperature creep behaviour. Common structural steel does not show any transient creep at room temperature since mobile dislocations are pinned down by the interstitial carbon atoms. The interstitial-free low carbon steel shows transient creep at room temperature since there are no free interstitials in the solid solution to form Cottrell atmospheres and to lock mobile dislocations.

The transient creep behaviour of austenitic stainless steels is explained by the very low mobility of interstitial atoms at room temperature. The diffusion coefficient for interstitial atoms in austenitic stainless steels is very low at room temperature compared to that in ferritic carbon steels. Therefore interstitial atoms are not able to form atmospheres at dislocations. In order to verify this theory, the authors carried out constant load creep tests at elevated temperature for SUS type 304 austenitic stainless steel. This approach was motivated by the fact that the mobility of interstitial atoms increases with increasing temperature. It was found that the creep rate decreases with increasing temperature. Finally, at $T = 300\,°C$, the transient creep vanished altogether, Figure 33. At this temperature, the diffusion coefficient of carbon in austenitic stainless steel is the same as that in ferrite (α-Fe) at room temperature, Figure 34. Therefore experiments corroborated the proposed theory.

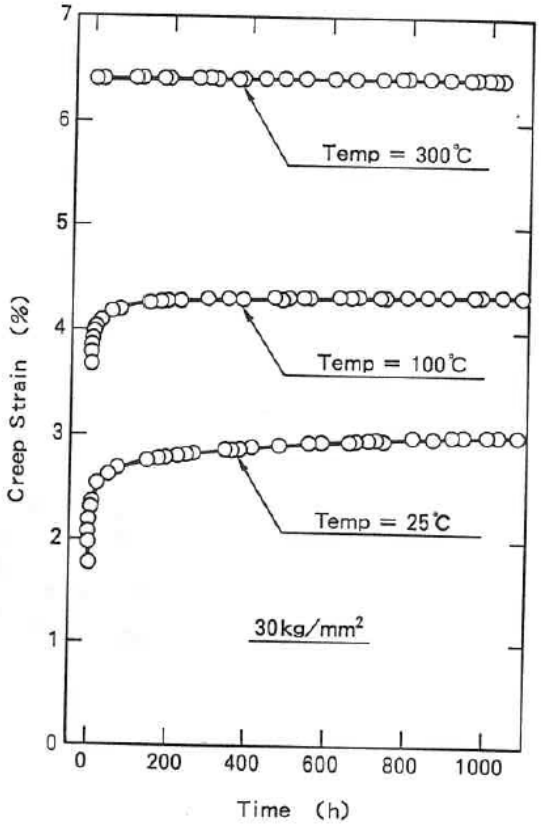

Figure 33. Creep curves for SUS 304 at room temperature and at elevated temperature [47].

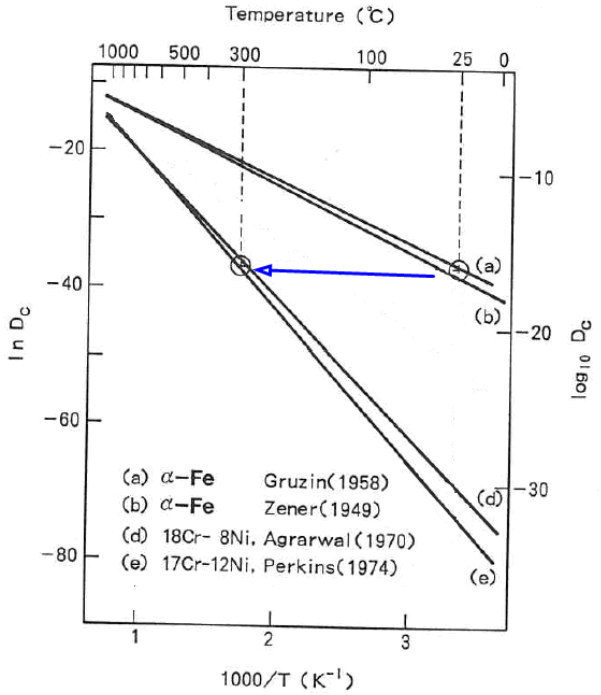

Figure 34. Diffusion coefficient for alpha iron and austenitic stainless steel. Adapted from [47].

6.8. Tendo, Yamada and Shimura

Tendo, Yamada and Shimura [48] studied creep and stress relaxation in bolted connections made of austenitic stainless steel. The purpose of this study was to quantify the stress relaxation due to creep deformation of austenitic stainless steel plates connected with high tension bolts. The experimental testing program consisted of constant load creep tests on plate materials and stress relaxation tests conducted on two different joint models. The bolts, washers and nuts were made of precipitation hardened martensitic stainless steel with yield strength of $R_{p0.2} > 1000$ *MPa*. The plates were SUS type 304 austenitic stainless steel with different strength levels. Two different strengthening methods, namely, nitrogen alloying and hardening by cold rolling were used.

Table 4. Test materials used by Tendo, Yamada and Shimura[48].

Grade	Condition	Rp0.2	Description
304	Annealed	265 MPa	Basic SUS 304
304N	Annealed	394 MPa	SUS 304 strengthened by nitrogen alloying
304	Cold-rolled	717 MPa	SUS 304 strengthened by cold-rolling

In the constant load creep tests material plate materials deformed according to the logarithmic creep law.

$$\varepsilon = \alpha \ln t \quad \Leftrightarrow \quad \dot{\varepsilon} = \frac{\alpha}{t} \tag{1}$$

The value of the creep parameter α was a linear function of applied stress, Figure 35. For the annealed plate materials of 304 and 304N -type, the stress dependency of α changes abruptly near the $R_{p0.2}$ proof stress level.

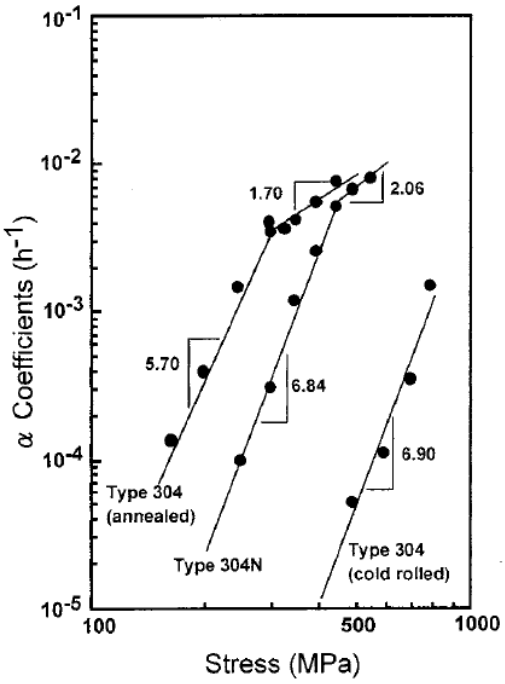

Figure 35. Stress dependency of creep parameter α for three SUS type 304 plate materials [48].

Stress relaxation in joints was studied using two different test setups. In the first joint model two ring-shaped specimens were piled and tightened using high tension bolt, nut and washers. The stress in the bolt was measured using a strain gage embedded in the bolt. The bolt was tightened manually by rotating the nut until the axial preload in the bolt shank reached 700 MPa. After the preloading the stress was allowed to relax. During the relaxation period both bold preload and the distance between the washers were measured for up to 700 hours. Figure 36 shows stress relaxation measured for annealed type 304 plate materials using this test setup. The axial stress in the bolt and the distance between the washers decreased with time. Therefore it can be concluded that the plate material crept under the compressive stress from the high tension bolts. The stress relaxation was significantly reduced when plate materials with higher yield strength was used, Figure 37.

In the second test setup, stress relaxation was studied in actual joints. In the joints, the splice plates were either annealed or cold rolled type 304 plates, Figure 38. The connected plates were always annealed. The bolts were preloaded like in the first test setup and the axial load in the bolts and the distance between the washers were measured in a similar manner as in the first setup. It was found that the stress relaxation could be significantly reduced by using splice plates hardened by cold rolling, Figure 39.

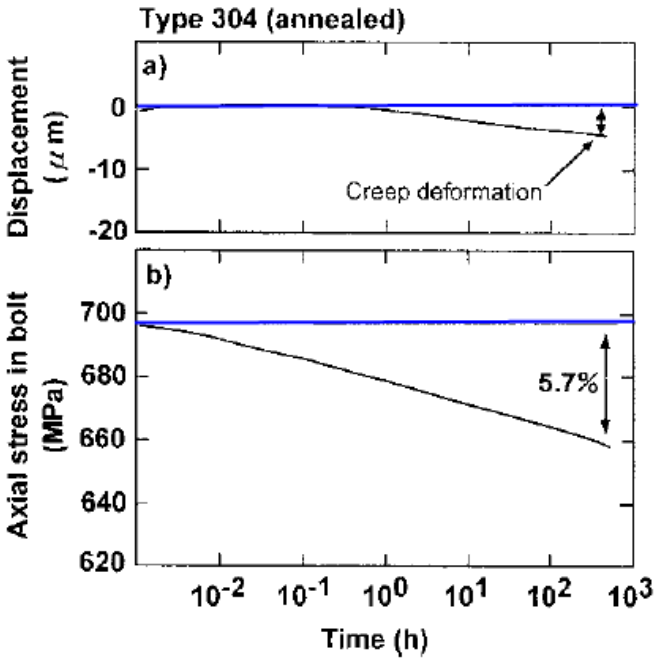

Figure 36. Stress relaxation in the first joint model with two piled ring shaped specimens made of annealed type 304 plates. Adapted from [48] .

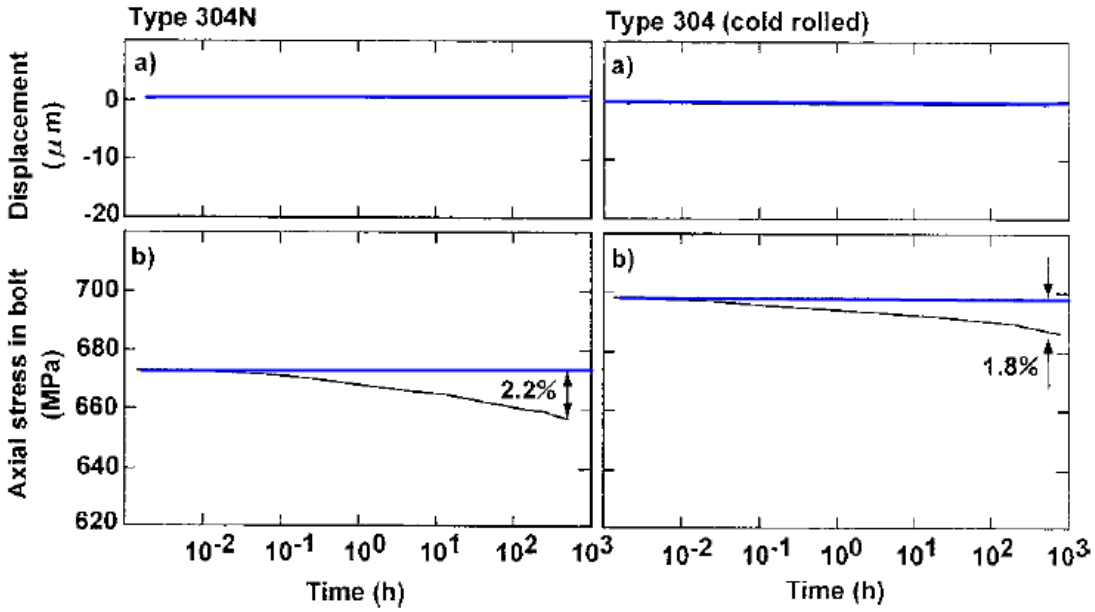

Figure 37. Stress relaxation in the first joint model with two piled ring shaped specimens made of nitrogen alloyed and cold rolled type 304 plates. Adapted from [48].

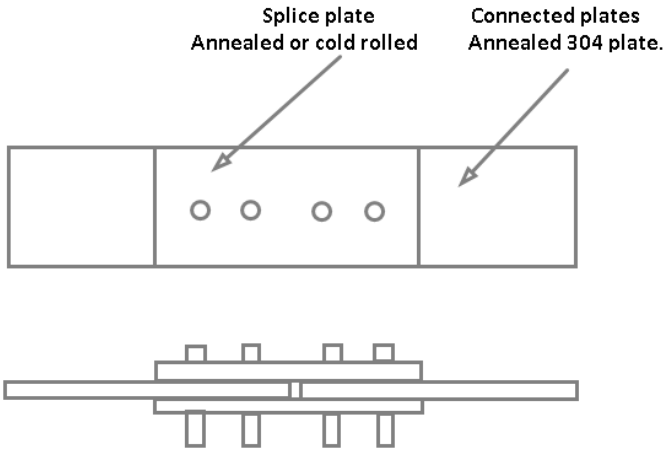

Figure 38. Schematic illustration of test setup number two employing actual friction type bolted connections.

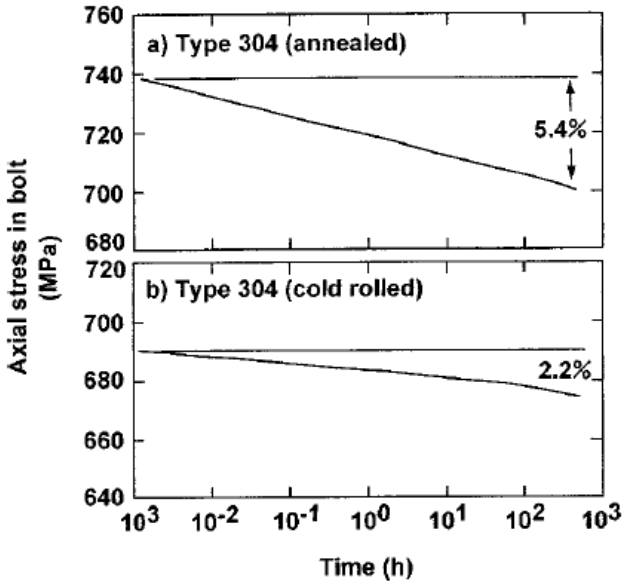

Figure 39. Change of axial bolt stress in actual bolted connection with two different types of splice plates [48]. The connected plates were annealed in both cases.

The stress relaxation in the connections was also studied using an axisymmetric finite element model. The bolt, nut and washers were modelled as elastic bodies. The deformation of plate material was considered to be additively composed of elastic, plastic and creep deformation. The plastic deformation was modelled using the von Mises yield condition, associative flow rule and a nonlinear isotropic hardening model. The isotropic hardening was determined using uniaxial tensile test results. The creep was modelled using the logarithmic creep law given by equation (1). The value of creep parameter α was bilinear as shown in Figure 35. The preloading of bolts was modelled by displacement boundary condition applied on the bolt end. The simulated results show that the creep deformation is concentrated around the bolt hole beneath the washer, Figure 40. Therefore the stress relaxation in the connection can be explained by creep deformation in this region. Furthermore, the stress relaxation was significantly reduced for type 304N splice plates due to the higher yield strength of this material.

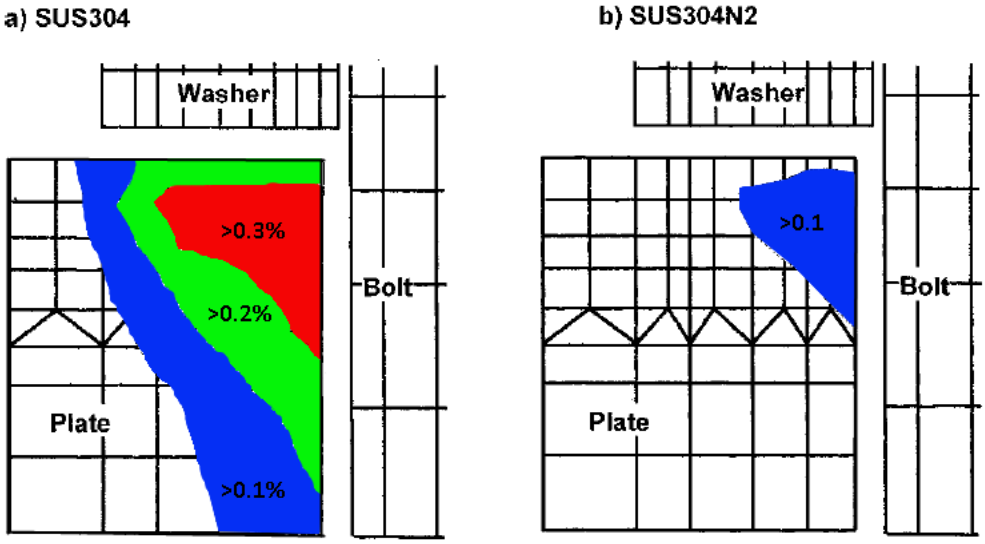

Figure 40. Calculated distribution of creep strain in bolted connections after 700 hours. Adapted from [48].

6.9. Usami and Mori

Usami and Mori [49] studied the creep deformation of austenitic stainless steel in the temperature range from -263°C to +200°C. Their research work was motivated by application of austenitic stainless steel in superconducting magnets. Eight austenitic stainless steels were used as test materials. Four test materials were standard austenitic grades and the other four high manganese and precipitation hardening grades. High strength Ni-Cr-Mo alloy steel 3.5NiMoV was included as a reference material. The mechanical properties of test materials are summarized in Table 5. The test material denoted by JIS SUS 304 was hardened by cold rolling. Tensile tests and creep tests were conducted using a servo-hydraulic tensile testing machine equipped with a thermostat and a cryostat.

Table 5. Mechanical properties of test materials studied by Usami and Mori [49].

Material	Rp0.2 (MPa)	Rm (MPa)	A (%)
JIS SUS 302	619	879	45
JIS SUS304	630	786	28.3
JIS SUS316L	265	570	62
JIS SUS316LN	313	657	52
5Mn12Ni21Cr2Mo	754	998	34.6
JIS SUH660	765	1116	23.6
15Mn16Cr	560	1052	31.8
18Mn18Cr	1050	1201	30.1
3.5NiMoV	575	717	26.5

Figure 41 shows creep test results for SUS 316L at room temperature. It can be observed that logarithmic creep does not continue throughout the whole testing period. It holds only up to $t = 10^4$ s. Thereafter the creep strain rates decrease more rapidly than that predicted by the logarithmic creep law, Figure 41(a). In the high stress region ($\sigma \approx R_{p0.2}$) the creep strain rate is proportional to the seventh power of stress. The exponent in the power law expressing the proportionality decreases smoothly with decreasing stress and becomes one at low stress region ($\sigma < 0.4\ R_{p0.2}$), Figure 41(b).

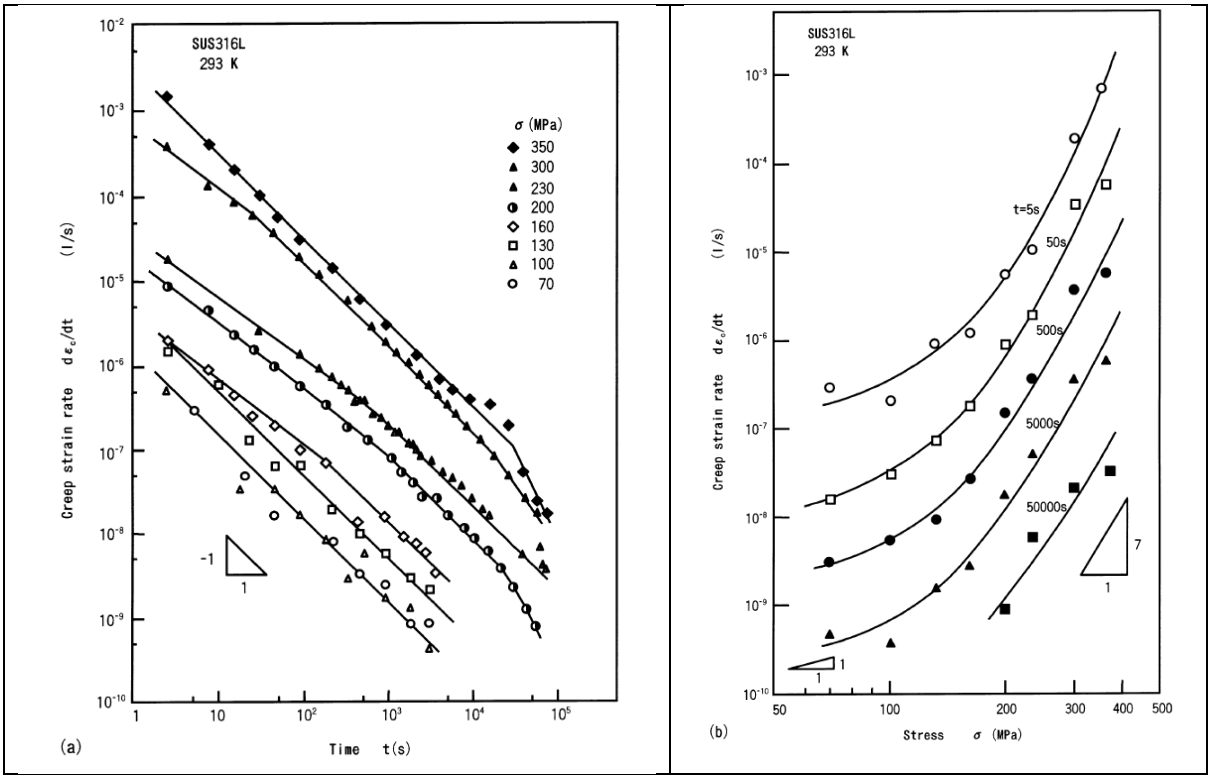

Figure 41. Creep strain rate for SUS 316L at room temperature as a function of time and as a function of applied loading in constant load creep tests [49].

In creep tests logarithmic creep was observed in every tested material. Every tested material also showed noticeable creep strain in the temperature range from -263°C to +200°C, Figure 42. Also the Cr-Ni-Mo alloy steel (3.5NiMoV) used as reference material showed noticeable creep deformation at low and medium temperatures. Therefore it was concluded that most structural metals show transient creep at the studied temperature range.

Concerning the temperature dependency of creep resistance, the authors found that the immediate plastic strain caused by the loading is a good indicator for the long term creep strain, Figure 43. The ratio of plastic strain and creep strain measured in a 10^5 second constant load creep test was fairly constant in the temperature range from -263°C to +100°C.

Usami and Mori also studied the influence of room temperature pre-straining on the creep behaviour. Specimens made of type 316L austenitic stainless steel were pre-strained to different stress levels ranging from 220 MPa to 240 MPa. After loading and unloading the same specimens were subjected to a constant load creep tests under 200 MPa loading. Figure 44 shows that the creep strain decreased and finally completely vanished with increasing pre-straining stress. This method was equally effective when the preloading was carried out at different temperature than the creep testing. Figure 45 summarizes the results for an experiment in which samples made of grade 316LN stainless steel were pre-strained at room temperature and subjected to creep testing at $T = -196°C$.

The final conclusion regarding the pre-straining experiments was that the creep deformation can be prevented by pre-straining the material with a plastic strain larger than that estimated to occur in the component under operating conditions. The pre-straining can be carried out in the fabrication phase at room temperature regardless of the operating temperature.

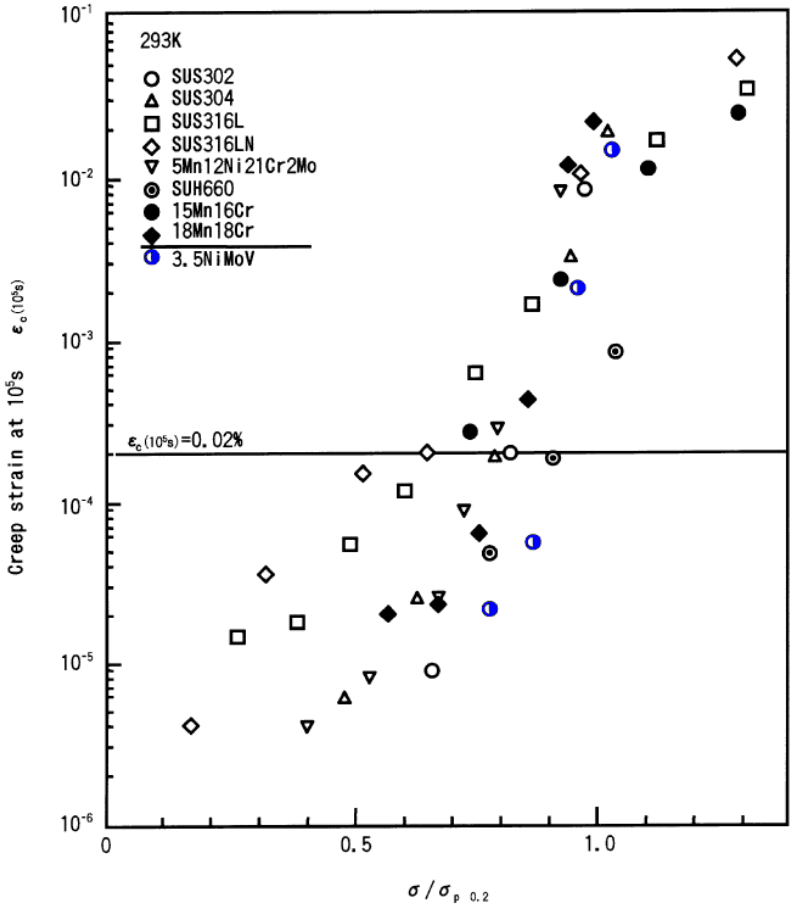

Figure 42. Creep strain after 10^5 s for all studied materials. Also the alloy steel (3.5NiMoV) used as reference material showed noticeable creep deformation. Adapted from [49].

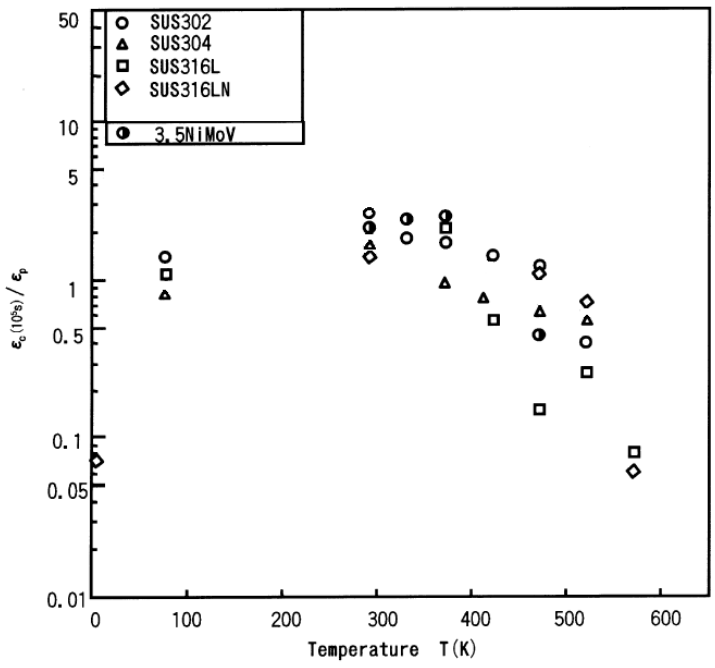

Figure 43. Ratio of plastic strain and creep strain after 10^5 second constant load creep test for selected austenitic stainless steels and the alloy steel used as reference material. Adapted from [49].

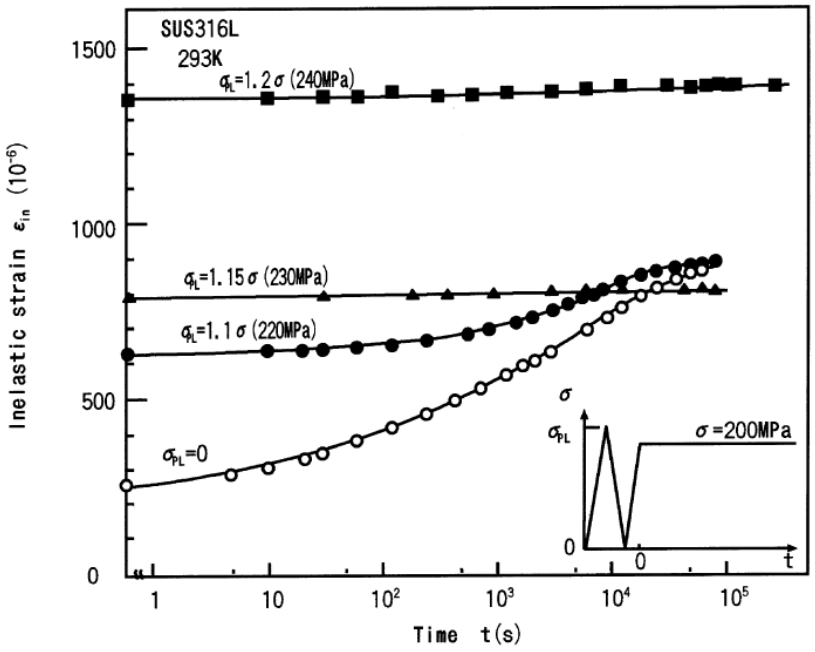

Figure 44. Influence of pre-strain on the creep behaviour of SUS 316L [49].

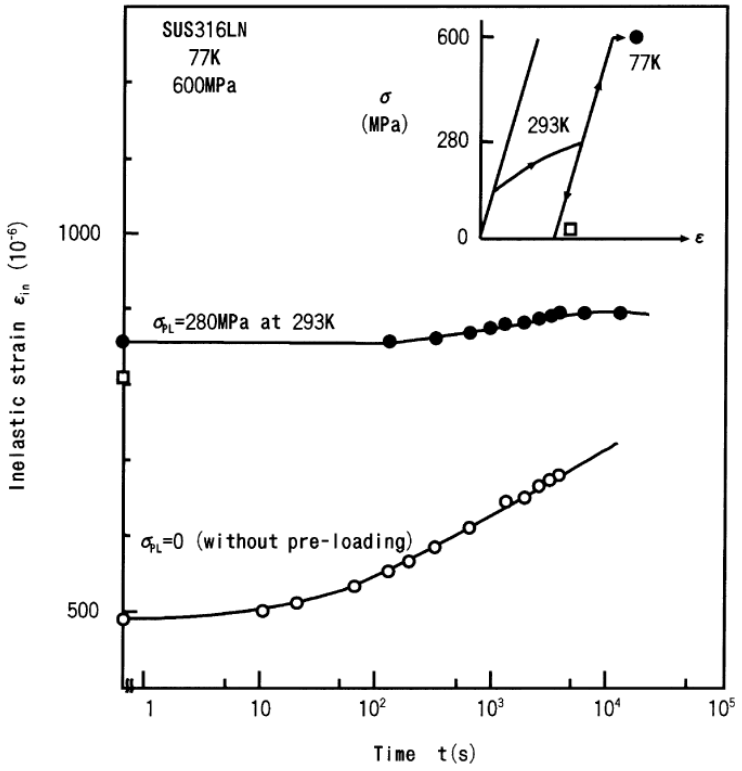

Figure 45. Effect of room temperature pre-straining on creep deformation at different temperature for SUS 316LN austenitic stainless steel [49].

6.10. Physically-based constitutive models

Physically-based constitutive models describe plasticity and creep deformation of polycrystalline metals based on the physical processes occurring during the deformation process. Physically-based models are founded on laws derived in the field of metal physics for the kinetics of dislocation motion in the presence of different types of obstacles. These models can be used to predict material behaviour over a wide range of temperatures and strain rates. Physically-based constitutive models typically have superior predictive power over phenomenological models. The major disadvantage of physically-based models is the large number of material parameters needed to describe the kinetics of dislocation motion and the interaction of dislocations with different types of obstacles. Physically based constitutive theories such as the Kocks-Mecking theory [50,51], the Estrin-Mecking theory [52,53] and the Mechanical Threshold Stress model [54] have been also used for predicting room temperature creep and stress relaxation behaviour of metals and alloys.

Tsuchida and his co-workers [55,56] made an extensive study on the mechanical behaviour of grade JIS SUS 310S austenitic stainless steel. The test material was subjected to variety of different mechanical tests. The experimental tests included:

- Basic tensile tests at different temperatures from -196°C to 25°C and strain rates from 10^{-5} to 10^{-2} (1/s).
- Tensile tests with a stepwise change of temperature or strain rate.
- Crosshead arresting tests, i.e. tensile tests with intermittent stress-relaxation periods.
- Constant load creep tests.

Figure 46 shows creep curves measured at room temperature creep using different stress levels. Logarithmic creep occurred over the whole time range except for the highest applied stress 546 MPa, Figure 47. The creep test results could be described using the following empirical model as a function of time and applied stress.

$$\dot{\varepsilon} = 10^{-13}\,\sigma^{2.7}\,t^{-1} \qquad (30)$$

The lines in Figure 47 were calculated with this equation. Crosshead arresting tests were carried out to measure the amount of stress relaxation during a 100-hour holding period at -196°C and at room temperature [56]. It was found that the amount of stress relaxation was independent of the plastic strain obtained before the holding period. No strain rate history effects were observed in the crosshead arresting tests. When the loading was increased between the holding periods, the measured stress-strain curve coincided with one measured in an uninterrupted tensile test.

In both articles [55,56] the observed material behaviour was modelled using the Kocks-Mecking theory [50,51]. In all cases, the stress strain response calculated with the Kocks-Mecking theory showed good correspondence with the measured material response. Therefore it was concluded that Kocks-Mecking theory can be used for modelling the stress strain response also at very low strain rates over a wide range of temperatures.

Follansbee applied the Mechanical Threshold Stress (MTS) model to predict the stress strain response of austenitic stainless steels [54,57,58]. The model was mainly used for predicting the stress-strain responses in tension or compression testing over a wide range of temperatures and strain rates.

The physically based constitutive models generally describe the strength of material being composed of contributions from different types of obstacles to dislocation motion. The observed flow stress can be therefore decomposed in components arising from grain boundaries (gb), solute atoms (sol) and dislocations (dis).

$$\tau = \tau_{gb} + \tau_{sol} + \tau_{dis} \qquad (31)$$

Dislocations overcome the obstacles by thermal activation. Since the obstacles form different energy barriers to be overcome by thermal activation, the rate dependency of each component in (31) is different. Grain boundaries are formidable obstacles to dislocation motion, and the strength component caused by the grain boundaries is generally believed to be temperature and strain rate independent. [54]

The physically-based theories therefore predict that creep and stress relaxation will cease if the stress caused by external loading falls below the threshold value determined by the grain size of the material. The strength contribution originating from grain boundaries can be estimated using the Hall-Petch equation [59].

$$\tau_{gb} = \frac{K}{\sqrt{d}} \qquad (32)$$

where *K* is a material dependent constant and *d* is the average grain diameter. According to Follansbee [54,57] the typical value of parameter *K* equals to $K = 433\ MPa\sqrt{\mu m}$ for a number of austenitic stainless steel grades.

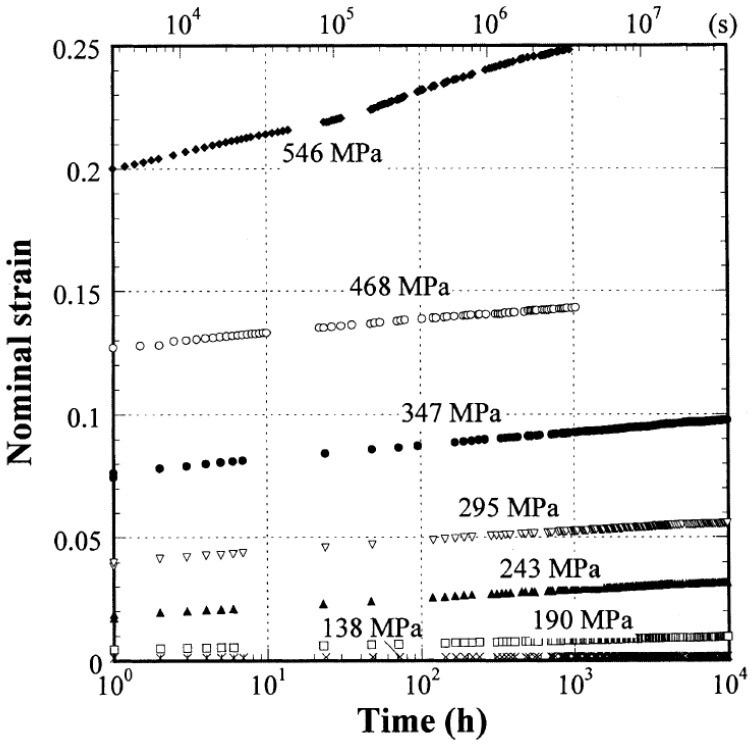

Figure 46. Constant load creep test results for grade SUS 310S test material [55].

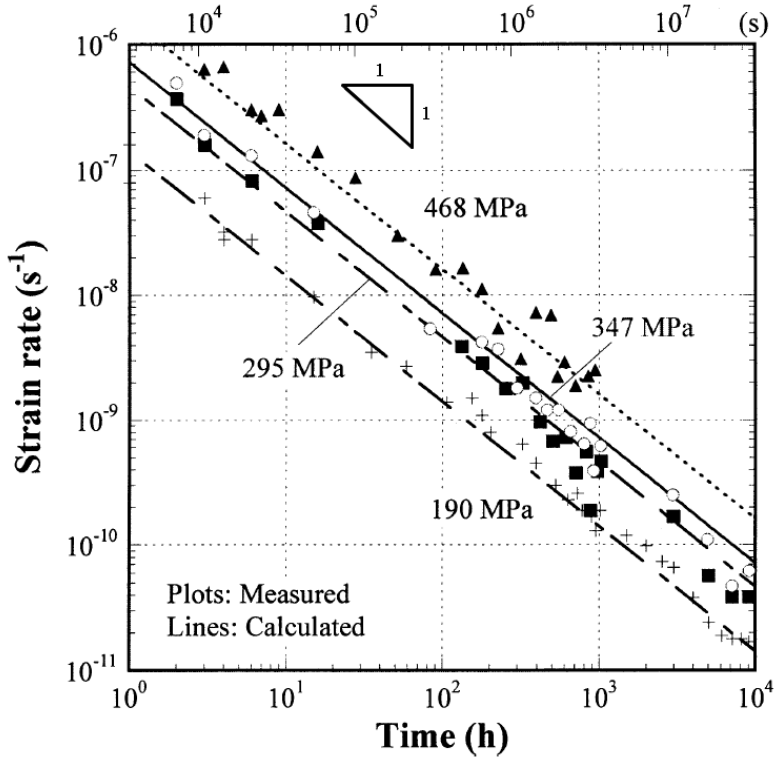

Figure 47. Creep strain rate as a function of time for grade SUS 310S test material. Adapted from [55].

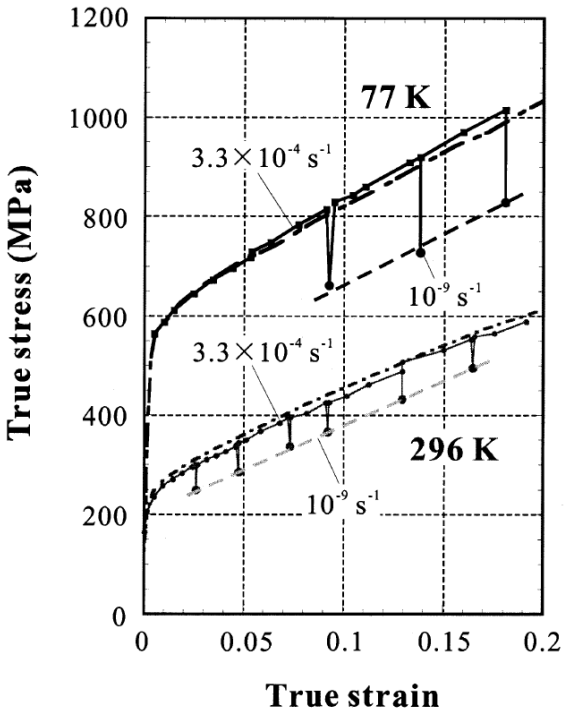

Figure 48. Crosshead arresting tests at -196°C and at room temperature for grade SUS 310S test material. The holding period was 100 hours. [56]

6.11. Krapf

Krapf studied stress relaxation in post-tensioned stainless steel rods in her master thesis [60]. Post-tensioned stainless steel rods are used for strengthening reinforced concrete pier caps under shear loading. Stress relaxation experiments were carried out on AISI type 304 rods using six different stress levels. The rods were hardened by cold working. The yield strength of studied rods was $R_{p0.2}$ = *670 MPa* and the tensile strength R_m = *830 MPa*. Relaxation tests were conducted using high stress values ranging from 92% to 96% of the tensile strength of the material. The experimental test results were modelled using the viscoplastic model proposed by Liu and Krempl [61]. The model predicted approximately 10% stress relaxation in 50 years. Furthermore, 80% of the stress loss occurred within the first hour of loading. Based on experimental and numerical results the design strength of *0.6* f_u was proposed for post-tensioned stainless steel rods.

6.12. Kassner and co-workers

Kassner, Geantil and Rosen [62] studied room temperature transient creep of AISI type 304 austenitic stainless steel using a lever-arm dead-weight creep testing equipment. The test material was either in annealed or in cold-worked state. In both cases the measured creep curves were could be successfully described using the logarithmic creep model

$$\varepsilon_p = \varepsilon_0 + \alpha \ln t \qquad (33)$$

The creep parameter β was modelled as a linear function of applied stress σ.

$$\alpha = a \cdot \sigma + b \qquad (34)$$

For the annealed material, two sets of parameters a and b were needed to describe the creep curves over the whole range of creep loads. The first set of values was determined for creep loads below the 0.2% proof stress and the second set above this level. Figure 49 shows constant load creep test results for the annealed material for creep loads below the 0.2% proof stress values. The longest testing period in Figure 49 was approximately 10 months and continuously increasing creep strains were measured over this whole testing period.

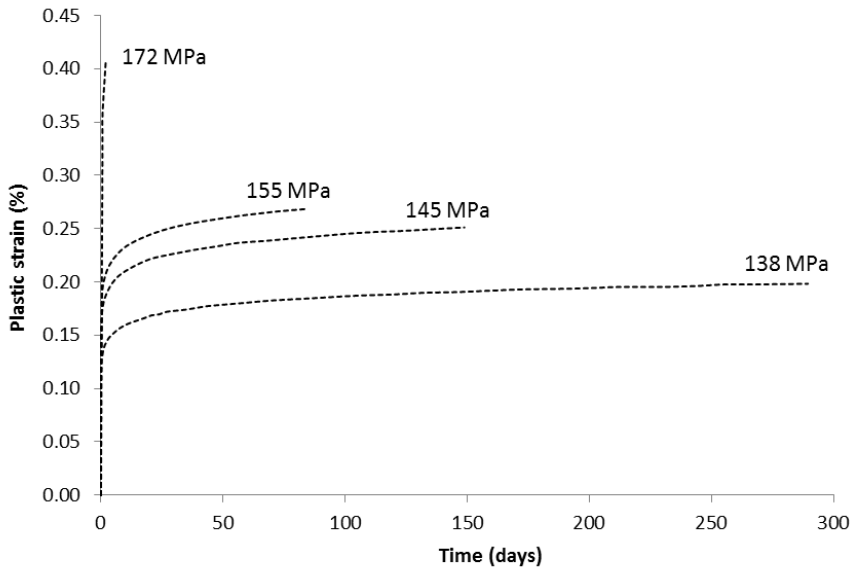

Figure 49. Creep curves measured for AISI type 304 austenitic stainless steel in annealed condition. The 0.2% proof stress of the material was 221 MPa. Adapted from [62].

It was also found that the creep resistance of cold-worked material was higher than that of the annealed material. Therefore it was concluded that ambient temperature creep can be effectively suppressed by cold-working.

In a recent review article Kassner and Smith discuss the low temperature creep behaviour of different pure metals and alloys [4]. They conclude that the creep curves can be described either by logarithmic or by power law creep for all studied materials. Steel and stainless steel showed logarithmic creep behaviour.

7. Creep and stress relaxation of duplex stainless steels

Low temperature creep tests were performed by Linder, Jargelius-Pettersson and Oscarsson [63] for duplex grades 2304, 2507 and 2205 and austenitic grades 316L and 316 LN in a servo hydraulic test machine at 100˚C. The creep loads were in the range from 60% to 120% of the 0.2% proof stress of the materials. The maximum creep period was 30 hours. The tests show that the duplex grades have slightly lower creep rate compared to the austenitic grades. The results are, however, of limited use since only data for stress versus time to creep rate below 10^{-8} 1/s and the deformation during the loading phase are presented.

Long-term room temperature creep tests were performed for grade 2205 duplex steel in 1992 at Outokumpu Avesta Research Centre [64]. The measured creep curves are shown in Figure 50. Creep curves for standard austenitic stainless steel grades are shown for reference. The results show that 2205 has similar creep behaviour as the AISI 304 denoted by letter D. The creep strain was approximately 0.3% after 10 hours and 0.45% after 100 hours for 2205 at 90% of the 0.2% proof stress of the material. Similar results were obtained in another study where room temperature creep tests were performed on large diameter bar and extruded seamless tubes in duplex stainless steel 2507 at 80%, 90% and 100% of the 0.2% proof stress of the material [65]. The results show relatively low creep deformation at 80% and 90% of the 0.2% proof stress; the creep strain was just below 0.4% after 1200 hours. In contrast, relatively high creep strains were observed at 100% of the 0.2% proof stress. In this case, the creep strain was approximately 2% after 1200 hours. The creep rate was high in the beginning of the creep test for all load levels. The creep rate, however, decelerated rapidly and there was almost no creep deformation after longer loading periods. The bar material showed higher degree of creep compared to the extruded tube material. This is likely caused by significantly higher austenite spacing in the bar material. Therefore a fine microstructure seems to be beneficial. The results for 2205, 304 and 304N also suggest that the logarithm of creep strain is a linear function of the ratio of applied stress to Rp0.2.

Boniardi, La Vecchia and Roberti [66] conducted stress relaxation tests on 11 mm 2205 duplex and on 15 mm type 2507 super duplex plates. The specimens were cylindrical with the diameter of $D = 8\ mm$ diameter and gauge length of $L = 25\ mm$. The cross-head speed was 0.5 mm/min in the loading phase. The relaxation time was at least 30 min. The results are summarized in Figures 51 and 52. Based on their experimental results, the authors conclude that the room temperature stress relaxation behaviour of these duplex grades can be described by a plastic equation of state according to Hart's theory. It was also concluded that the austenite phase in principle governs the stress relaxation phenomenon.

In the work of Kivisäkk and Chai [67], two types of duplex stainless steels were tested at 200°C by using U-bent specimens according to ASTM G30. The stress level was equal to the yield strength at the test temperature. After 1000 hours the stress relaxation of UNS S32304 was 17 % while that of UNS S32205 was 12 % stress.

Bar and extruded tube made of grade UNS S32750 duplex stainless steel were tested in slow strain rate machine at room temperature [68]. No significant stress relaxation was found for the two product forms. This was explained by the low loading level used. The loads used were in the range from 47% to 63 % of the 0.2% proof stress of the material.

Triplicate stress relaxation tests were made on grade 2205 and 2304 duplex strands by Schuetz [69]. The stress loss was 2.49% for the 2205 strand after 1000 hours at initial stress level which corresponds to 74 % of the 0.2% proof stress of the material. For the 2304 strand the stress loss was 2.07 % at initial stress level which corresponds to 43 % the 0.2% proof stress of the material.

Material	Proof stress (N/mm^2)	Composition								
		C	Si	Mn	P	S	Cr	Ni	Mo	N
A (304N)	362	0.04	0.61	1.50	0.012	0.017	19.0	8.9	0.06	0.27
B (304N)	283	0.046	0.48	1.55	0.010	0.015	18.0	8.7	0.05	0.16
C (304)	239	0.035	0.49	1.55	0.030	0.010	18.3	9.0	0.42	0.08
D (304)	316	0.050	0.38	0.99	0.025	0.002	18.2	8.3	0.15	0.05
E (Duplex 2205)	483	0.017	0.39	1.49	0.019	0.001	22.2	5.75	2.96	0.20

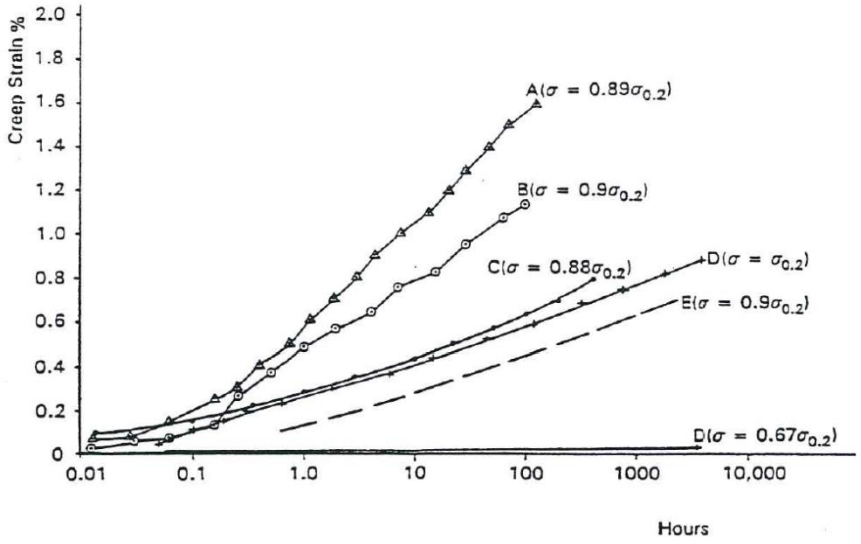

Figure 50. Long term room temperature creep of 304N, 304 and 2205 at 89%, 90% and 100 % of Rp0.2

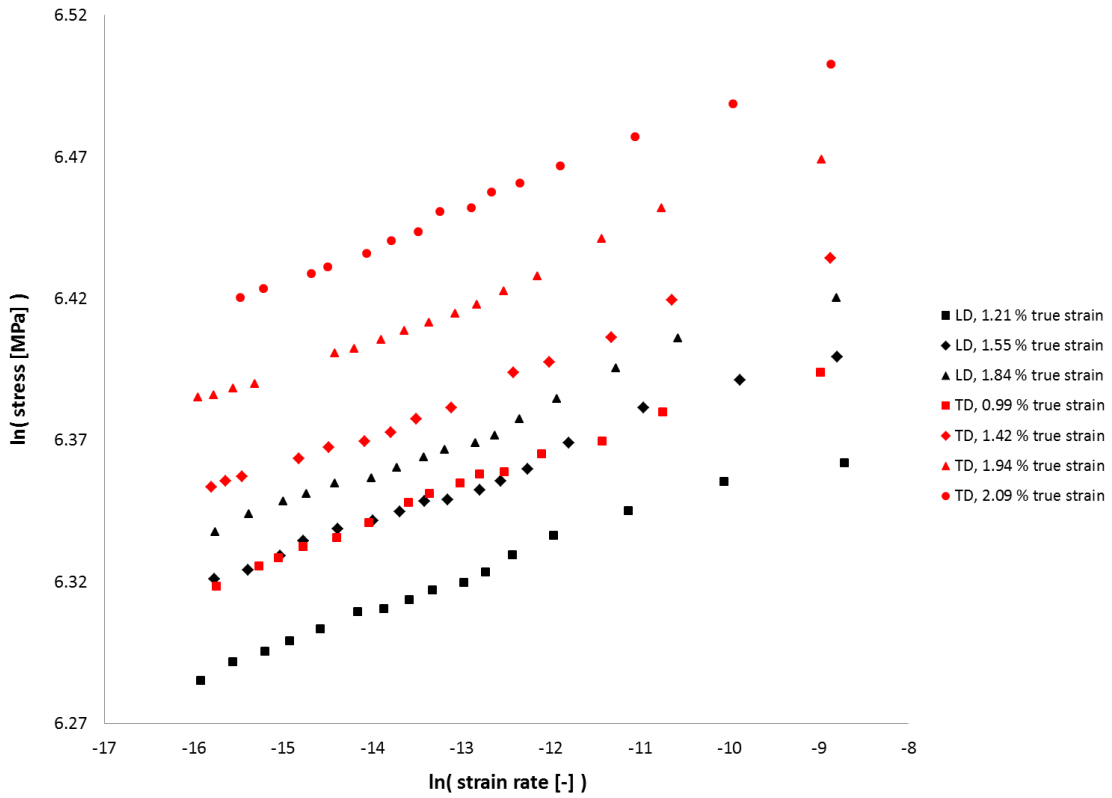

Figure 51. Stress-relaxation in type 2205 duplex steel in longitudinal (LD) and transverse (TD) direction. The loading in terms on true strain in the beginning of the relaxation is given in the legend.

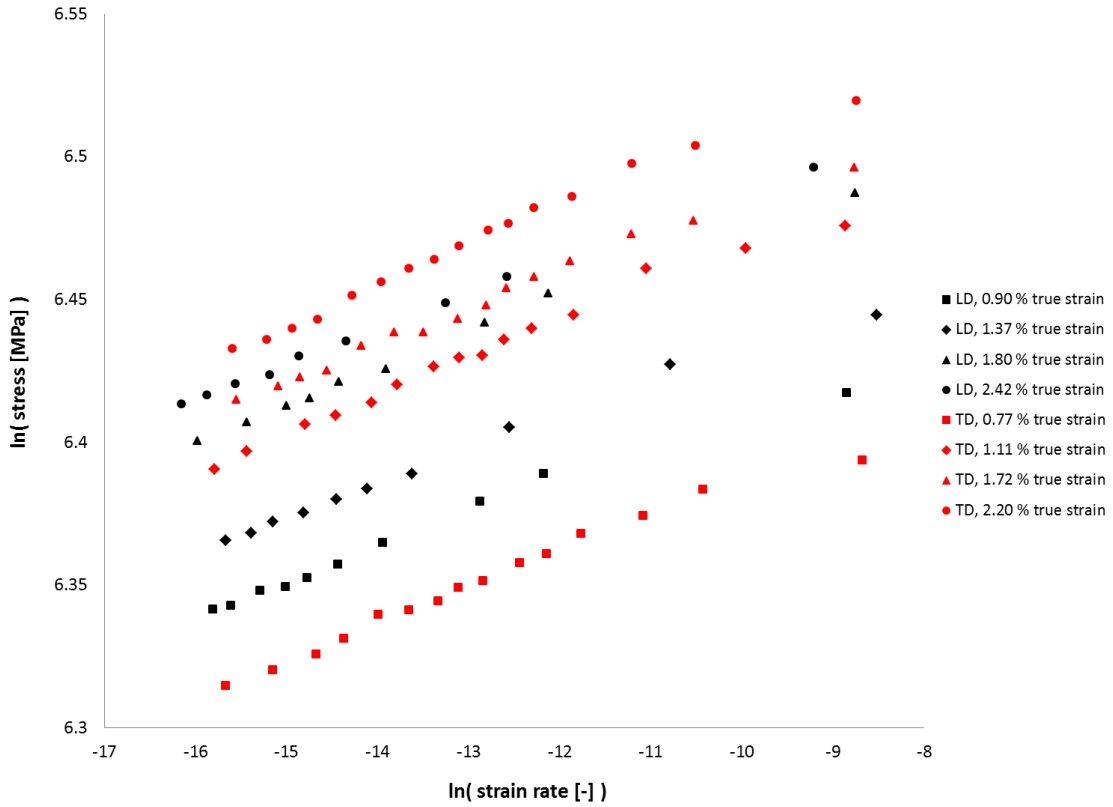

Figure 52. Stress-relaxation in type 2507 super duplex steel in longitudinal (LD) and transverse (TD) direction. The loading in terms on true strain in the beginning of the relaxation is given in the legend.

The results on duplex grades can be summarized as follows:

- The room temperature stress relaxation of the duplex stainless steels can be described using a plastic equation of state according to Hart's theory.
- The austenite phase governs the stress relaxation phenomenon for the duplex stainless steels.
- The amount of stress relaxation was different in different duplex grades. This was most likely caused by notable differences in the yield strength of different duplex grades.
- The amount of stress relaxation was different in the longitudinal direction compared to that in the transverse direction.
- It seems that the product form has no influence on the stress relaxation phenomenon. This observation may be, however, also explained by the low load used for the testing.

8. Creep and stress relaxation of other types of steel

According to the World Steel Association there are over 3500 different steel grades. Steel grades can be classified in four different groups:

- Carbon steels.
- Alloy steels.
- Stainless steels.
- Tool steels.

As discussed in chapter 2, the physical mechanism responsible for creep and stress relaxation at low temperature in all steels is dislocation glide. Furthermore, the rate of creep deformation is dictated by the rate by which dislocations, assisted by thermal activation, are able to surmount different types of obstacles. Since the physical mechanism is the same in all steels, this literature study was extended to cover also recent studies on other groups of steels.

Schmidt and von den Steinen made comparative studies [43–45] on the room temperature creep characteristics of steels with different crystal structures and different microstructures. The test materials included common structural steel, quenched and tempered steel and martensitic steel. They found that there are no fundamental differences between steels with ferritic, austenitic or martensitic crystal structure. It was concluded that other factors than the crystal structure control the room temperature creep behaviour. Specifically, it was found that materials with distinct upper and lower yield point showed very little transient creep deformation when loaded sufficiently below their upper yield point. When loaded at or above certain critical limit, the same materials showed significant transient creep deformation.

Tendo, Takeshita, Nakazawa and Abo [47] studied the room temperature creep characteristics of common structural steel and interstitial-free low carbon steel. In ferritic materials, the sharp yield point is typically caused by the locking of dislocations by interstitial atoms. Therefore interstitial-free low carbon steel does not have a sharp yield point. When room temperature constant load creep tests were carried out on both materials, the interstitial-free low carbon steel showed considerable transient creep. The transient creep behaviour of interstitial-free steel was similar to that of austenitic stainless steel. It was concluded that the interaction of dislocations with interstitial atoms and the resulting formation of sharp yield point plays an important role in the room temperature creep behaviour.

Similar findings have been also reported by Wang, Zhang and Chen on pipeline steels [71]. Depending on chemical composition and processing condition, pipeline steels have a stress-strain curve either with or without a sharp yield point. Pipeline steels with both types of yielding behaviour were subjected to constant load creep test. The creep tests were divided in two categories. If the creep load was sufficiently low in order not to cause any immediate plastic deformation in the test piece in the loading stage, the test was termed ‘pre-yield creep test’. And if the creep load caused measurable immediate plastic deformation in the test piece in the loading stage, the test was termed ‘post-yield creep test’. It was found that all studied steels showed significant transient creep in the post-yield creep tests. In contrast, in the pre-yield creep tests, the creep characteristics were strongly dependent on the type of yielding behaviour. In the presence of a sharp yield point, only minimal creep deformation was observed. In the absence of a sharp yield point, however, relatively large creep deformation occurred in the pre-yield creep tests.

The post-yield creep behaviour of nine different metallic materials studied by Jordan and Freed [71]. The set of test materials included two titanium alloys, low carbon steel, austenitic stainless steel, copper, brass and three aluminium alloys. Significant post-yield transient creep was observed in eight of the nine tested materials. In some cases the post-yield room temperature creep resulted in a failure of the specimen in the test. It was concluded that the majority of common metals exhibit significant post-yield creep deformation at room temperature.

The room temperature creep characteristics of high strength steels was studied by Oehlert and Atrens [20] and by Liu, Liu, Zhao and Northwood [72]. The high strength steels studied did not exhibit a sharp yield point. In both cases, significant creep deformation was observed with stress levels below the 0.2% proof stress.

The results of survey on the creep and stress relaxation behaviour of different types steels at room temperature therefore suggest that existence of a sharp yield point plays in important role in the room temperature creep of steel. The yield point phenomenon generally occurs in steels containing interstitial atoms such as carbon and nitrogen in solid solution. The rearrangement of interstitial around dislocations leads locking dislocations in their positions. This locking and unlocking of dislocations explains the formation upper yield point in materials such as common structural steel. However, once released from solute atmospheres, dislocations are able to move under lower external loading. This explains the drop of yield stress once the upper yield point has been surpassed. [73]

Room temperature transient creep is also caused by movement of dislocations. Therefore it is evident that the locking of dislocations by solute atmospheres and the subsequent formation of sharp yield point also prevents room temperature creep deformation. It can be argued that dislocation locking constitutes an energy barrier that needs to be surmounted before the creep deformation can proceed. Only once this barrier is overcome, may the creep process be activated.

It is, however, worth noting that the creep limit of materials with a sharp yield point is not equal to the upper or lower yield point measured in a standard tensile test. The upper and lower yield points depend on the loading rate used in the tensile testing. Under sustained creep loading, the loading rate approaches zero. Therefore, the theoretical creep limit equals to the upper yield point measured in an infinitely slow tensile test. Further on, different types of microscopic and macroscopic stress concentrations may locally trigger the unlocking of dislocations at a stress level that is lower than the theoretical creep limit defined above. Therefore the practical creep limit should be considered equal to the loading level that does not cause any immediate plastic deformation in the presence of realistic amount of imperfections and stress concentrations.

The results on the creep and stress relaxation of other types of steel can be generalized as follows:

- Steels with a sharp yield point do not show transient creep provided that the load is below the elastic limit and does not cause any immediate plastic deformation in the loading stage.
- Steels with a sharp yield point show considerable transient creep if the creep load exceeds elastic limit and therefore causes at least certain immediate plastic deformation in the material.
- All steels with gradual yielding show transient creep when loaded above their elastic limit.

9. Summary

In this literature study, available information on creep and stress relaxation behaviour of stainless steel at room temperature was reviewed. The characteristics of creep and stress relaxation behaviour of different types of stainless steels were discussed. Also potential mathematical models for describing the creep deformation in preloaded slip-resistant bolt connections made of stainless steel were reviewed.

The most important findings can be summarized as follows:

I. The physical mechanism responsible for creep and stress relaxation at low temperature in all types of steel is dislocation glide. The creep rate is dictated by the rate by which dislocations are able to surmount different types of obstacles assisted by thermal activation.

II. There are no fundamental differences in the room temperature creep behaviour of materials with different crystal structure. Test materials with martensitic (BCT), ferritic (BCC) and austenitic (FCC) crystal structure behave in a qualitatively similar manner in the room temperature creep tests.

III. The creep behaviour is controlled by two characteristic values called the creep limit and the creep resistance. Both variables are related to the tensile stress-strain behaviour of the material. The creep limit determines the upper limit for purely elastic behaviour. No creep or stress relaxation may occurs below this stress level. The creep resistance defines how the creep deformation decelerates. The creep resistance is determined the instantaneous slope of the true stress vs. true plastic strain curve determined at the point in which the creep deformation starts. A rapid work hardening results in rapid deceleration of the creep deformation.

IV. The creep limit generally increases with increasing yield strength of the material.

V. The creep limit increases when material is plastically deformed. It follows that the creep deformation can be minimized by cold-working the material before the creep loading.

VI. The different methods that can be used for strengthening materials are not equivalent. Solid solution hardening by nitrogen or carbon alloying was less efficient way of increasing the creep resistance than hardening by cold-rolling.

VII. The creep and stress relaxation behaviour depends strongly on the loading rate. The amount the creep and stress relaxation increase with increasing loading rate.

VIII. Material work hardens during room temperature creep. The work hardening caused by creep equals to that observed in tensile testing.

IX. Viscoplastic models based on overstress between the current stress and quasistatic flow stress can be used for describing most of the observed phenomena.

X. The room temperature creep of stainless steels was frequently described as logarithmic creep.

XI. In a joint model, the creep deformation concentrated under the bolt head and nut. Furthermore, the loss of bolt preload could be significantly reduced by using cover plates hardened by cold rolling.

XII. The existence of upper and lower yield points seems to play an important role in the room temperature creep characteristics of all types of steel. All steels with smooth, gradual yielding show similar transient creep as stainless steel. Only steels that possess a sharp upper and lower yield point do not creep at room temperature when loaded below their elastic limit.

10. References

[1] J.C. Gibeling, Creep Deformation of Metals, Polymers, Ceramics and Composites, in: H. Kuhn, D. Medlin (Eds.), ASM Handbook, Volume 8: Mechanical Testing and Evaluation, ASM International, Materials Park, Ohio, 2000: pp. 363–368.
[2] J.C. Earthman, Introduction to Creep and Stress-Relaxation Testing, in: ASM Handbook, Volume 8: Mechanical Testing and Evaluation, ASM International, 2000: pp. 361–362.
[3] J.W. Jones, Theory of Creep Deformation, in: ASM Metals Handbook, Ninth Edition, 1st ed., American Society of Metals, Metals Park, Ohio, 1985: pp. 308–310.
[4] M.E. Kassner, K. Smith, Low temperature creep plasticity, Journal of Materials Research and Technology. 3 (2014) 280–288.
[5] R.E. Smallman, Modern Physical Metallurgy, 4th ed., Butterworths, 1985.
[6] F. Garofalo, Fundamentals of Creep and Creep Rupture in Metals, Macmillan Co., New York, 1965.
[7] O.H. Wyatt, Transient Creep in Pure Metals, Nature. 167 (1951) 866.
[8] H.J. Frost, M.F. Ashby, Deformation-Mechanism Maps, The Plasticity and Creep of Metals and Ceramics, 1st ed., Pergamon Press, 1982.
[9] S.J. Zinkle, G.E. Lucas, Deformation and Fracture Mechanisms in Irradiated fcc and bcc Metals, US Department of Energy, 2003.
[10] E. Orowan, The Creep of Metals, Journal of the West of Scotland Iron and Steel Institute. 54 (1947) 45–96.
[11] C.L. Smith, A Theory of Transient Creep in Metals, Proceedings of the Physical Society. 61 (1948) 201–205.
[12] F.R.N. Nabarro, The time constant of logarithmic creep and relaxation, Materials Science and Engineering. A309-310 (2001) 227–228.
[13] F.R.N. Nabarro, H.L. de Villiers, The Physics of Creep - Creep and Creep Resistant Alloys, 1st ed., Taylor & Francis, London, 1995.
[14] A.H. Cottrell, Logarithmic and Andrade creep, Philosophical Magazine Letters. 75 (1997) 301–307.
[15] M.A. Korhonen, S.-P. Hannula, C.-Y. Li, Workhardening Correlations Based on State Variables in Some FCC Metals in Monotonic Loading, Metallurgical Transactions A. 16A (1985) 411–420.
[16] E. da C. Andrade, On the viscous flow in metals, and allied phenomena, Proceedings of the Royal Society of London. Series A, Containing Papers of a Mathematical and Physical Character. (1910) 1–12.
[17] N.S. Ottosen, M. Ristinmaa, The mechanics of constitutive modeling, Elsevier, 2005.
[18] R.K. Penny, D.L. Marriott, Design for creep, Springer Science & Business Media, 2012.
[19] K. Santaoja, Lecture Notes on Continuum Thermomechanics, Helsinki University of Technology, Laboratory for Mechanics of Materials, Helsinki, 2006.
[20] A. Oehlert, A. Atrens, Room temperature creep of high strength steels, Acta Metallurgica et Materialia. 42 (1994) 1493–1508.
[21] J. Lemaitre, J.-L. Chaboche, Mechanics of solid materials, Cambridge university press, 1994.
[22] A.D. Freed, J.-L. Chaboche, K.P. Walker, A viscoplastic theory with thermodynamic considerations, Acta Mechanica. 90 (1991) 155–174.
[23] E.W. Hart, C.-Y. Li, H. Yamada, G.L. Wire, Phenomenological theory: a guide to constitutive relations and fundamental deformation properties, Constitutive Equations in Plasticity. 171 (1975) 149–197.
[24] E.W. Hart, Constitutive relations for the nonelastic deformation of metals, Journal of Engineering Materials and Technology. 98 (1976) 193–202.
[25] J.L. Chaboche, G. Rousselier, On the plastic and viscoplastic constitutive equations - Part I : Rules developed with internal state variable concept, Journal of Pressure Vessel Technology. 105 (1983) 153–158.
[26] E.W. Hart, Load relaxation testing and material constitutive relations, in: A. Fox (Ed.), Load Relaxation Testing, ASTM STP 676, ASTM, 1979: pp. 5–20.
[27] J.H. Holbrook, J.C. Swearengen, R.W. Rohde, Specimen-Test Machine Coupling and Its Implications for Plastic Deformation Models, in: R.W. Rohde, J.C. Swearengen (Eds.), Mechanical Testing for Deformation Model Development, ASTM STP 765, ASTM, 1982: pp. 80–101.
[28] J.D. Whittenberger, Creep, Stress-Rupture, and Stress-Relaxation Testing. Introduction, in: Metals Handbook, 9th ed., American Society of Metals, 1985: pp. 301–307.
[29] S.P. Hannula, M.A. Korhonen, C.Y. Li, Strain aging and load relaxation behavior of type 316 stainless steel at room temperature, Metallurgical and Materials Transactions A. 17 (1986) 1757–1767.
[30] S.-P. Hannula, C.-Y. Li, Repeated load relaxations of type 316 austenitic stainless steel, Scripta Metallurgica. 18 (1984) 225–229.
[31] D.W. Henderson, R.C. Kuo, C.-Y. Li, The applicability of Hart's state variable model to large strain rate ranges, Scripta Metallurgica. 18 (1984) 1021–1023.
[32] I. Gupta, J.C.M. Li, Stress relaxation, internal stress, and work hardening in some BCC metals and alloys, Metallurgical Transactions. 1 (1970) 2323–2330.

[33] H. Yamada, C.-Y. Li, Stress relaxation and mechanical equation of state in austenitic stainless steels, Metallurgical Transactions. 4 (1973) 2133–2136.
[34] M.A. Korhonen, S.-P. Hannula, C.-Y. Li, Workhardening correlations based on state variables in some FCC metals in monotonic loading, Metallurgical Transactions A. 16 (1985) 411–420.
[35] N. Nir, F.H. Huang, E.W. Hart, C.-Y. Li, Relationship between anelastic and nonlinear viscoplastic behavior of 316 stainless steel at low homologous temperature, Metallurgical Transactions A. 8 (1977) 583–588.
[36] F.H. Huang, F.V. Ellis, C.-Y. Li, Comparison of Load Relaxation Data of Type 316 Austenitic Stainless Steel With Hart's Deformation Model, Metallurgical Transactions A. 8A (1977) 699–704.
[37] J.F. Thomas, F.L. Yaggee, Stress relaxation in solution-annealed and 20 pct cold-worked type 316 stainless steel, Metallurgical and Materials Transactions A. 6 (1975) 1835–1837.
[38] E. Krempl, An experimental study of room-temperature rate-sensitivity, creep and relaxation of AISI type 304 stainless steel, Journal of the Mechanics and Physics of Solids. 27 (1979) 363–375.
[39] D. Kujawski, V. Kallianpur, E. Krempl, An experimental study of uniaxial creep, cyclic creep and relaxation of AISI Type 304 stainless steel at room temperature, Journal of the Mechanics and Physics of Solids. 28 (1980) 129–148.
[40] E. Krempl, V.V. Kallianpur, Some Critical Experiments For Viscoplasticity at Room Temperature, Journal of the Mechanics and Physics of Solids. 32 (1984) 301–314.
[41] E. Krempl, H. Lu, The hardening and rate-dependent behavior of fully annealed AISI type 304 stainless steel under biaxial in-phase and out-of-phase strain cycling at room temperature, Journal of Engineering Materials and Technology. 106 (1984) 376–382.
[42] H.-C. Wu, C.-C. Ho, Strain hardening of annealed 304 stainless steel by creep, Journal of Engineering Materials and Technology. 115 (1993) 345–350.
[43] W. Schmidt, A. von den Steinen, Besonderheiten des Kriechens von Stählen bei Raumtemperatur, Materialprüfung. 14 (1972) 183–191.
[44] W. Schmidt, A. von den Steinen, Untersuchung des kriechverhaltens bei Raumtemperatur von Stählen mit unterschidlichem Gefügeaufbau und Festigkeitsverhalten, Achiv Für Das Eisenhüttenwesen. 42 (1971) 479–488.
[45] W. Schmidt, A. von den Steinen, Zum Kriechverhalten einiger Stähle bei Raumtemperatur, Materialprüfung. 11 (1969) 83–89.
[46] W. Schmidt, H. Dietrich, Einfluss einer Katlverformung aud den Zusammenhang zwischen Raumtemperaturkriechen und Bauschinger-Effect, Thyssen Edelst. Techn. Ber. 7 (1981) 41–54.
[47] M. Tendo, T. Takeshita, T. Nakazawa, H. Abo, Room Temperature Creep Behavior of Austenitic Stainless Steels, in: Proceedings of International Conference on Stainless Steels 1991, ISIJ, Chiba, Japan, 1991: pp. 487–493.
[48] M. Tendo, K. Yamada, Y. Shimura, Stress relaxation behavior at high-tension bolted connections of stainless-steel plates, Journal of Engineering Materials and Technology. 123 (2001) 198–202.
[49] S. Usami, T. Mori, Creep deformation of austenitic steels at medium and low temperatures, Cryogenics. 40 (2000) 117–126.
[50] H. Mecking, U.F. Kocks, Kinetics of flow and strain-hardening, Acta Metallurgica. 29 (1981) 1865–1875.
[51] U. Kocks, H. Mecking, Physics and phenomenology of strain hardening: the FCC case, Progress in Materials Science. 48 (2003) 171–273.
[52] Y. Estrin, H. Mecking, A unified phenomenological description of work hardening and creep based on one-parameter models, Acta Metallurgica. 32 (1984) 57–70.
[53] Y. Estrin, Dislocation theory based constitutive modelling: foundations and applications, Journal of Materials Processing Technology. 80 (1998) 33–39.
[54] P.S. Follansbee, Fundamentals of Strength—Principles, Experiment, and Application of an Internal State Variable Constitutive Model. the Minerals, Metals, & Materials Society, John Wiley & Sons, Inc., Hoboken. (2014).
[55] N. Tsuchida, E. Baba, O. Umezawa, K. Nagai, Y. Tomota, True stress-true strain relations with very low strain rates at room temperature for an austenitic 25Cr-19Ni steel, ISIJ International. 44 (2004) 209–213.
[56] N. Tsuchida, Y. Tomota, H. Moriya, O. Umezawa, K. Nagai, Application of the Kocks–Mecking model to tensile deformation of an austenitic 25Cr–19Ni steel, Acta Materialia. 49 (2001) 3029–3038.
[57] P.S. Follansbee, An internal state variable constitutive model for deformation of austenitic stainless steels, Journal of Engineering Materials and Technology. 134 (2012) 041007.
[58] P.S. Follansbee, Structure Evolution in Austenitic Stainless Steels—A State Variable Model Assessment, Materials Sciences and Applications. 6 (2015) 457.
[59] D. Hull, D.J. Bacon, Introduction to dislocations, 5., Butterworth-Heinemann, 2011.
[60] C. Krapf, Stress relaxation of post-tensioned stainless steel rods for bridge pier cap shear strengthening, MSc thesis, Georgia Institute of Technology, 2010.
[61] M.C.M. Liu, E. Krempl, A uniaxial viscoplastic model based on total strain and overstress, Journal of the Mechanics and Physics of Solids. 27 (1979) 377–391.

[62] M.E. Kassner, P. Geantil, R.S. Rosen, Ambient Temperature Creep of Type 304 Stainless Steel, Journal of Engineering Materials and Technology. 133 (2011).
[63] J. Linder, R.F.A. Jargelius-Pettersson, A. Oscarsson, Low temperature creep in austenitic and duplex stainless steels, Institute of Metals, Sweden, 2001.
[64] H. Groth, Room temperature creep of 2205. Research Report, Avesta Research Centre, Avesta, Sweden, 1992.
[65] U. Kivisäkk, Relation of room temperature creep and microhardness to microstructure and HISC, Materials Science and Engineering: A. 527 (2010) 7684–7688.
[66] M. Boniardi, G.M. La Vecchia, R. Roberti, Stress relaxation behaviour in duplex and superduplex stainless steels, in: Proceedings of the Fourth International Conference Duplex Stainless Steels, Glasgow, Scotland, 1994.
[67] U.H. Kivisäkk, G. Chai, Influence of test method and relaxation on the result from stress corrosion cracking tests of stainless steels in dilute neutral chlorides, Corrosion. 59 (2003) 828–835.
[68] U. Kivisäkk, Investigation Of Low Temperature Creep And Relaxation Behaviour Of Stainless Steels At Stress Levels Representative For Hydrogen Embriltlement, in: CORROSION 2007, NACE International, 2007.
[69] D.P. Schuetz, Investigation of high strength stainless steel prestressing strands, MSc thesis, Georgia Institute of Technology, 2013.
[70] S.-H. Wang, Y. Zhang, W. Chen, Room temperature creep and strain-rate-dependent stress-strain behavior of pipeline steels, Journal of Materials Science. 36 (2001) 1931–1938.
[71] E.H. Jordan, A.D. Freed, Room-temperature post-yield creep, Experimental Mechanics. 22 (1982) 354–360.
[72] C. Liu, P. Liu, Z. Zhao, D.O. Northwood, Room temperature creep of a high strength steel, Materials & Design. 22 (2001) 325–328.
[73] R. Abbaschian, L. Abbaschian, R.E. Reed-Hill, Physical Metallurgy Principles, Cengage Learning, Stamford, USA, 2008.